Project No. 13-5415

ORIGEN-based Nuclear Fuel Inventory Module for Fuel Cycle Assessment

Fuel Cycle Research and Development

Steven Skutnik
University of Tennessee at Knoxville

Kenneth Kellar, Federal POC
E.A. Hoffman, Technical POC

NEUP Nuclear Energy University Programs
U.S. Department of Energy

AWARD NUMBER: DE-NE0000737

ORIGEN-BASED NUCLEAR FUEL INVENTORY MODULE FOR FUEL CYCLE ASSESSMENT FINAL PROJECT REPORT

June 19, 2017

Steven E. Skutnik, Ph.D. (PI)
sskutnik@utk.edu
University of Tennessee-Knoxville
Department of Nuclear Engineering
DUNS number: 00-338-7891
Grant period: 1/2014–12/2017

Executive Summary

The goal of this project, "ORIGEN-based Nuclear Fuel Depletion Module for Fuel Cycle Assessment" is to create a physics-based reactor depletion and decay module for the Cyclus nuclear fuel cycle simulator in order to assess nuclear fuel inventories over a broad space of reactor operating conditions. The overall goal of this approach is to facilitate evaluations of nuclear fuel inventories for a broad space of scenarios, including extended used nuclear fuel storage and cascading impacts on fuel cycle options such as actinide recovery in used nuclear fuel, particularly for multiple recycle scenarios. The advantages of a physics-based approach (compared to a recipe-based approach which has been typically employed for fuel cycle simulators) is in its inherent flexibility; such an approach can more readily accommodate the broad space of potential isotopic vectors that may be encountered under advanced fuel cycle options.

In order to develop this flexible reactor analysis capability, we are leveraging the Origen nuclear fuel depletion and decay module from SCALE to produce a standalone "depletion engine" which will serve as the kernel of a Cyclus-based reactor analysis module. The ORIGEN depletion module is a rigorously benchmarked and extensively validated tool for nuclear fuel analysis and thus its incorporation into the Cyclus framework can bring these capabilities to bear on the problem of evaluating long-term impacts of fuel cycle option choices on relevant metrics of interest, including materials inventories and availability (for multiple recycle scenarios), long-term waste management and repository impacts, etc.

Developing this Origen-based analysis capability for Cyclus requires the refinement of the Origen analysis sequence to the point where it can reasonably be compiled as a standalone sequence outside of SCALE; i.e., wherein all of the computational aspects of Origen (including reactor cross-section library processing and interpolation, input and output processing, and depletion/decay solvers) can be self-contained into a single executable sequence. Further, to embed this capability into other software environments (such as the Cyclus fuel cycle simulator) requires that Origens capabilities be encapsulated into a portable, self-contained "library" which other codes can then call directly through function calls, thereby directly accessing the solver and data processing capabilities of Origen.

Additional components relevant to this work include modernization of the reactor data libraries used by Origen for conducting nuclear fuel depletion calculations. This work has included the development of new fuel assembly lattices not previously available (such as for CANDU heavy-water reactor assemblies) as well as validation of updated lattices for light-water reactors updated to employ modern nuclear data evaluations. Additionally, our analysis has sought to characterize and bound the level of uncertainty introduced through the use of unmodified fuel assembly lattice templates without specific features such as burnable poisons and soluble boron. Our findings indicate that over 85% of the variation in fuel assembly isotopes are attributable to burnup alone, indicating that these pre-generated libraries produce reasonably accurate representations of fuel assemblies for rapid depletion calculations. Further, this work found that the lattices used as the basis for Origen reactor data libraries generally are capable of reproducing isotopic

inventories measured from specific pins (i.e., during destructive radiochemical assay) with an accuracy generally to within 10% for an unaltered lattice. In particular, these lattices showed the best agreement for pins closest to the "assembly-average" spectrum (that is, far away from local features which adversely impact the flux spectrum, such as proximity to burnable absorbers or water holes).

An additional unexpected discovery during the implementation of this workscope was in the uncovering of a potential discrepancy in the ^{154}Eu thermal-region radiative capture cross-section, which was discovered during the process of validating the performance of the modernized ORIGEN being developed as a part of this workscope. This discovery has far-reaching impacts for areas including used fuel management (both in terms of radiation source terms and non-destructive measurement of burnup) as well as for used fuel safeguards. Our findings indicate that the current nuclear data libraries (ENDF/B-VII.0 and VII.1) appear to substantially underestimate the thermal-region neutron capture cross-section for ^{154}Eu, therefore resulting in consistent, signficant over-predictions of ^{154}Eu inventories in depletion calculations.

During this project phase, the main development work on this project has been in finalizing the necessary infrastructure to develop the ORIGEN-based reactor archetype for CYCLUS (CYBORG) and commencing development tasks for the CYCLUS-facing features. This has included finalizing all necessary improvements to the ORIGEN code base (which were subsequently released as part of the SCALE 6.2 release), development of a material storage facility for CYCLUS, and development of an initial release of the ORIGEN-based reactor archetype for CYCLUS.

The CYBORG reactor analysis module as-developed is fully capable of dynamic calculation of depleted fuel compositions from all commercial U.S. reactor assembly types as well as a number of international fuel types, including MOX, VVER, MAGNOX, and PHWR CANDU fuel assemblies. In addition, the ORIGEN-based depletion engine allows for CYBORG to evaluate novel fuel assembly and reactor design types via creation of ORIGEN reactor data libraries via SCALE. The establishment of this new modeling capability affords fuel cycle modelers a substantially improved ability to model dynamically-changing fuel cycle and reactor conditions, including recycled fuel compositions from fuel cycle scenarios involving material recycle into thermal-spectrum systems.

1 Accomplishments for 2016-2017

During the 2016-2017 performance period, we completed the initial development and testing of the proposed Nuclear Fuel Inventory Module – now termed CYBORG (**Cy**clus **B**ased **ORIG**EN). Essential aspects of this work include developing a code infrastructure that allows for lightweight coupling between ORIGEN and CYCLUS via an ORIGEN-CYCLUS interface layer which acts as an intermediary to the ORIGEN Application Program Interface (API). This interface layer translates CYCLUS-specific datatypes into C++ primitives and retrieves ORIGEN data back into a format that can readily be conveyed into CYCLUS recipe objects. The structure of this coupling allows users to directly compile against ORIGEN binary shared libraries (i.e., without requiring direct access to the ORIGEN source code - only headers and shared libraries), thereby obviating difficulties introduced by the export-controlled status of the SCALE code system by allowing users to leverage ORIGEN methods without exposing source code. In addition, CYBORG employs a modern build system using CMake, allowing it to easily be built on any system where SCALE and CYCLUS already reside.

Further, significant progress was made in the development of a problem-dependent means for ORIGEN reactor data library reduction, wherein isotopes and transitions that are of relatively little consequence to the problem metrics evaluated (e.g., decay heat, gamma emissions, radiotoxicity) are eliminated, reducing the size of the reactor data library and substantially improving the performance of depletion calculations. In addition to targeting a minimization of the computational penalty for employing physics-based depletion within CYCLUS, this method offers a number of substantial spillover benefits to a variety of advanced modeling and simulation capabilities. The goal of this work is to provide a physically rigorous means of transition matrix reduction which therefore as much as possible preserves the original problem physics. In as much, potential application areas include integration into areas such as the NEAMS toolkit for fuel performance applications (i.e., by reducing the computational cost of depletion within high-fidelity reactor simulations for depletion and fission product gas buildup, etc.) as well as other applications where direct integration of rigorous depletion may be desirable (such as with the UNFST&DARDS workflow for used fuel storage calculations as well as facility process monitoring and safeguards models).

As of this report's writing, a scale demonstration of problem-dependent reactor data library reduction has been performed, although additional work is being carried out using graph theory-informed approaches to optimize the selection of nuclides for elimination while preserving the essential physical features of the system.

1.1 Review of goals from prior performance period

During the last project performance period, major goals for the final project development period were to finalize the development of an initial release version of the ORIGEN-based Nuclear Fuel Inventory Module for CYCLUS and to continue the development of problem-dependent ORIGEN

library compression to reduce the computational costs of employing physics-based depletion. At present, an initial version of the CyBORG module for Cyclus is tested and functional, capable of calculating fuel depletion for a variety of fuel recipes and assembly types. In addition, significant progress has been made on the problem-dependent Origen library compression technique which promises to offer benefits not only to this project but to other embedded applications of Origen within the DOE-NE advanced modeling and simulation portfolio, including areas such as the NEAMS toolkit.

2 Major project accomplishments

2.1 Development of N-dimensional reactor data library interpolation

- **Targeted completion date (revised):** September 2015
- **Task completion status:** 100%

2.1.1 Background on interpolation of Origen reactor data libraries

In order to facilitate rapid depletion calculations using the most accurate nuclear data possible, ORIGEN calculations frequently make use of the ARP module to interpolate reactor data libraries to problem-specific conditions, thereby obviating the need to perform computationally-expensive lattice physics transport calculations for each depletion problem. Previous versions of SCALE up through SCALE 6.1 have provided a reactor data library interpolation capability through the ARP module [16, 11]. ARP defines three different types of interpolation conditions:

1. **LWR reactor data libraries**, which afford interpolation over the average assembly enrichment and void fraction, along with interpolation over each cycle's cumulative burnup,
2. **MOX fuel libraries**, with interpolation as a function of the average fractional ^{239}Pu within the plutonium, the average fraction of plutonium in the heavy metal content of the fuel, the average void fraction, and the average burnup for each cycle, and
3. **Activation libraries** in which users can interpolate over the total target fluence (i.e., accounting for target depletion).

The premise behind choosing these fixed interpolation parameters (i.e., average assembly enrichment, void fraction, ^{239}Pu enrichment, Pu fraction, and burnup) lies in the fact that the effective one-group absorption coefficients for important actinides generally vary slowly as a smooth function of these parameters, shown as Figures 1 and 2 [16]. Meanwhile, for MOX fuel, compositions for ^{238}Pu, ^{240}Pu, ^{241}Pu, and ^{242}Pu have been found to be well-correlated with ^{239}Pu; studies by ORNL have thus found that parameterization of the MOX fuel cross-sections solely on ^{239}Pu provides sufficient accuracy with minimal differences compared to a full parameterization of the plutonium isotopic vector [6].

Thus, problem-dependent cross-sections (such as the effective one-group absorption cross-sections and the transition matrix coefficients used to describe the Bateman equations) can be interpolated along these dimensions to produce problem-specific cross-sections with minimal loss of accuracy.

However, a limitation of the existing interpolation capability provided through the ARP module is that interpolation is limited to a set of fixed parameters, such as initial enrichment, moderator density, and burnup for UO_2 fuel assemblies. Similarly, the ARP-based system requires registration of the individual library characteristics through a text-based database, `arpdata.txt`, which lists

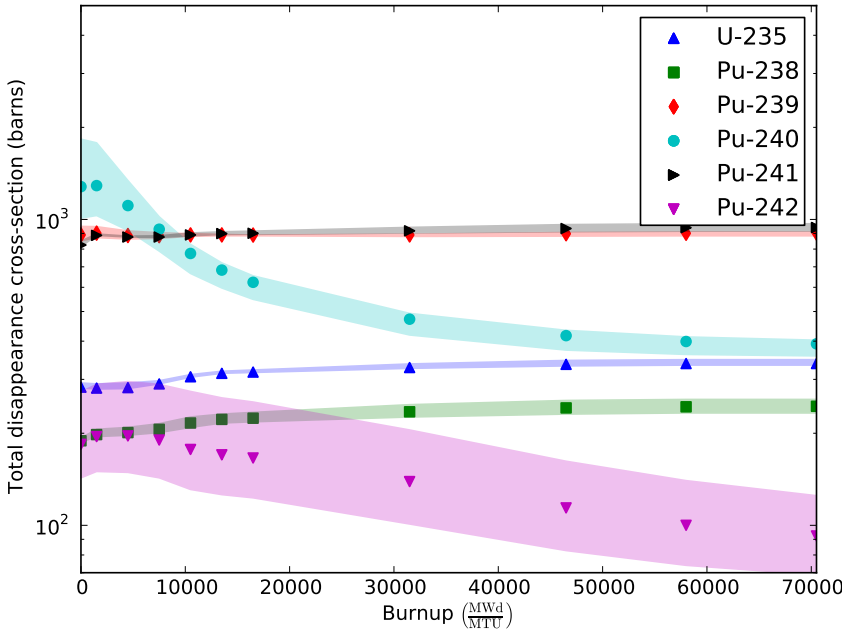

Figure 1: Total neutron disappearance cross-section as a function of burnup and void fraction for a GE 10x10-8 BWR assembly; filled areas represent the space of void values ranging from 10% to 90% (points indicate 50% void fraction) for a fixed average assembly enrichment of 3.0%.

the library interpolation points and all on-disk files corresponding to a particular library type. As an alternative

2.1.2 Development of a more portable, self-describing approach to Origen libraries

In order to obtain the desired level of flexibility and portability, especially in terms of the capability to handle user-specified interpolation dimensions at problem runtime, a new `TagManager` object a has been to the ORIGEN library format. This object holds a library of tags having two types: descriptive ID tags, which describe overall characteristics of a library (e.g., assembly type and other parameters used to select libraries for interpolation), and interpolable tags. This latter type of tag describes parameters that can be used to establish reference points for interpolation, such as enrichment, void fraction, fuel temperature, or any other type of continuous value. Interpolable tags consist of key-value pairs in the form of a name, (in the form of a standard string), and a value in the form of a double-precision floating point value. These are used to uniquely identify the point in the N-dimensional parameter space that the library represents.

As the interpolable tags afford a generalized interpolation capability, the ID tags make this capability accessible. For each major variation in a reactor assembly type, ARP would require

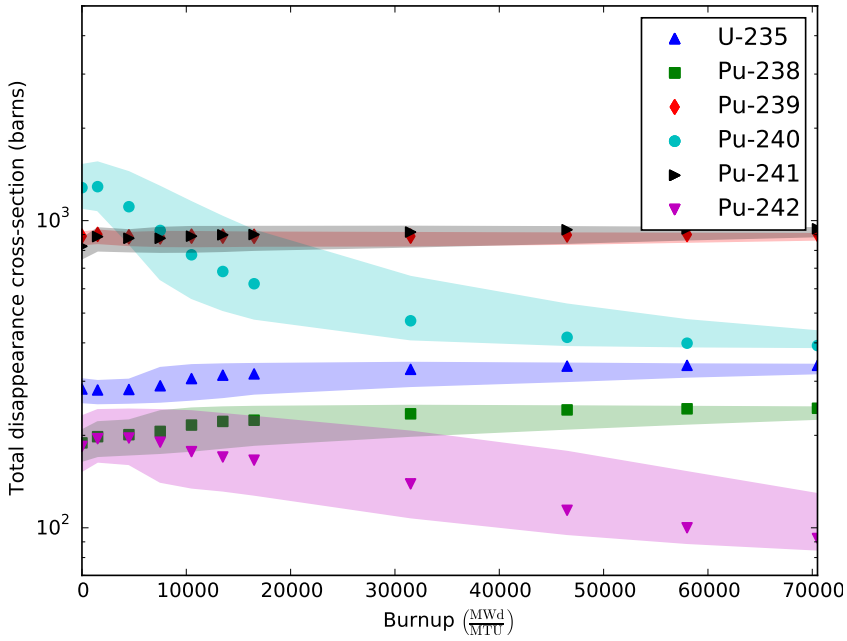

Figure 2: Total neutron disappearance cross-section as a function of burnup and enrichment for a GE 10x10-8 BWR assembly; filled areas represent the space of enrichment values ranging from 1.5% to 6% (points indicate 3% enrichment) for a fixed average assembly enrichment of 50%.

the libraries to have filenames specifying the value that library had for each dimension and an ever-expanding `arpdata.txt` file to reflect these assembly types, assuming it gained the ability to cover arbitrary dimensions. This quickly becomes untenable. ID tags allows for each library to tell a user everything he or she would need to know about it as well as quickly sorting through a large number of libraries in order to only select only those needed for the problem.

2.1.3 Generalized N-D interpolation approach

With the libraries and interpolation parameter space defined, a method of organizing the data such that the nearest neighbors can be determined for interpolation and their relative contributions is required. To achieve this goal, the `GridData` object was devised. `GridData` allows for the creation of an N-dimensional grid with ordered sets of data such that the i^{th} data set for every library are associated and can be referenced together. `GridData` constructs an N-dimensional space by defining "extents" in each interpolation dimension, comprised of the values for which data already exist. Across the parameter space, a set of "responses" can be defined where each response is composed of a data set at each location in the parameter space, allowing all of the data sets in a given response to be manipulated as one.

With this `GridData` object populated with data, a combination of weights across each dimension can be applied to combine the data in useful ways. For example, using a linear weighting, only the nearest neighbors in each dimension are given non-zero weights in developing the interpolated response values, minimizing the amount of data required for performing interpolation. This is especially important for the nuclide transition matrix $\overline{\overline{A}}$, which can consist of approximately 54,000 elements for each unique parameter configuration (e.g., enrichment, void fraction, and burnup combination).

To understand the application of N-D interpolation in practice, consider a two-dimensional system where the state is $\overrightarrow{x} = [u_i, v_j]$ with $i = 1 \ldots N_1$ (first dimension) and $j = 1 \ldots N_2$ (second dimension). With polynomial-based interpolation (which includes Lagrangian polynomials such as is employed by ARP [16]), the ideal solution is:

$$\overline{\overline{A}}\left(u', v'\right) = \sum_i c_i\left(u'\right) \sum_j c_j\left(v'\right) \overline{\overline{A^s_{(i,j)}}} \tag{1}$$

where the coefficients c_i and c_j are based only upon u' and v', respectively. Expressed differently, one can imagine a two-dimensional mesh of points composed of the states u and v, i.e., each point (u,v) represents a permutation of states in u and v. Any interpolated point (u', v') falls somewhere within the mesh between two nodes defined by $\left[u_i, u_{(i+1)}\right]$ and similarly $\left[v_j, v_{(j+1)}\right]$. Thus, the factors c_i and c_j can be thought of as dimensional "weights" between interpolation points in dimensions i and j.

This scheme avoids passing the large data sets $\overline{\overline{A}}$ through the interpolation algorithm as the coefficients may be calculated directly from the grid definition u and v and the desired values u' and v'. Further, data sets that do not participate in interpolation can easily be identified as those where $c = 0$ and a needless multiplication operation by zero can be avoided. As the number of dimensions grows, so too does the number of data sets; however, this technique provides the minimum amount of data operations required for interpolation.

2.1.4 Generalized interpolation performance benchmarks

Figure 3 shows a comparison of the interpolation performance between ARP and Obiwan (**O**rigen **B**inary file **I**nformation **W**hich **A**lso does **N**-dimensional interpolation, the command-line utility for library tag management and N-D interpolation) for a GE 7x7-0 BWR assembly. The enrichment and moderator density were chosen to be the same as those found on the preexisting ARP libraries so that no interpolation would occur over those dimensions. The only interpolation used in this figure is over burnup to show a fine resolution analysis of the performance of the three interpolation methods used by obiwan (nearest neighbor, linear, and cubic spline) as compared to ARP. The figure shows the greatest difference between any of the $> 50,000$ nuclide transitions tracked in these libraries at each burnup. As expected, the nearest neighbor method gives the greatest deviations from ARP, especially early in the cycle (where changes in the effective removal cross-sections are occurring more rapidly as a function of burnup), and at points furthest from

the burnups present on the pre-calculated libraries (labeled on the x-axis). Three points indicate a calculated percent difference of 35-55%, while most remain around or below 15%. Linear interpolation performs much better with a maximum calculated percent difference around 10%, also early in the cycle. Cubic spline interpolation performs the best with a maximum calculated percent difference of about 3.5%. Cubic spline is able to most closely match the results of ARP across the burnup values than both linear and nearest neighbor. The differences observed between cubic spline interpolation by obiwan and the fourth-order Lagrangian interpolation of ARP are expected given the differences in interpolation techniques.

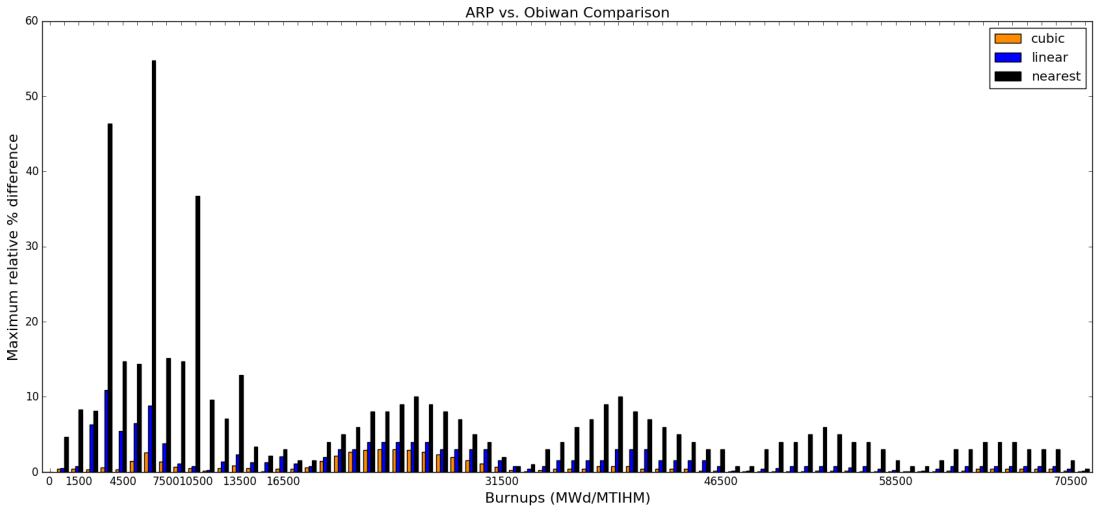

Figure 3: Comparison of the three interpolation methods of Obiwan to ARP. The labeled burnups indicate the burnups that exist on the precalculated libraries. The values indicate the greatest difference between any given cross section calculated by ARP and the various methods of obiwan. These calculations interpolated only over burnup.

Similar comparisons were performed that include linear interpolation over enrichment, moderator density, and both enrichment and moderator density. Similar results are observed in all cases. Analysis of the average differences shows that the maximums in the examples are extreme cases and for the most part, the average difference significantly less than the maximums.

A further comparison with TRITON was also conducted. TRITON is a sequence in SCALE that iterates between a transport-based neutron balance calculation to determine the multigroup flux and a material depletion calculation based on a collapsed one-group version of the calculated flux. A simulation was run using the ENDF/VII.0 238-group cross sections to construct a library using the burnups found in the Origen reactor data libraries on any SCALE installation for the GE 7x7-0 BWR fuel assembly. A second simulation was run using the fine burnup structure of the previous versions. Obiwan was used with the various interpolation techniques on the first run to generate a library with the fine burnup structure. This was then compared against the second

TRITON run on a transition-by-transition basis. The absolute disparity is not greater than that observed in the comparisons with ARP, but some percent differences are due to comparisons with incredibly small values (on the order of 10^{-10} barns or smaller). The ^{135}Xe absorption cross section was one of the largest absolute differences in all of the comparisons. Figure 4 shows the absorption cross section for this particular problem as a function of burnup. Figure 5 shows the absolute differences in the absorption cross section for ^{135}Xe as calculated by TRITON and Obiwan. Even though the absolute value of the difference is great, the percent difference shows that it is a relatively small difference compared to the magnitude of the cross section itself.

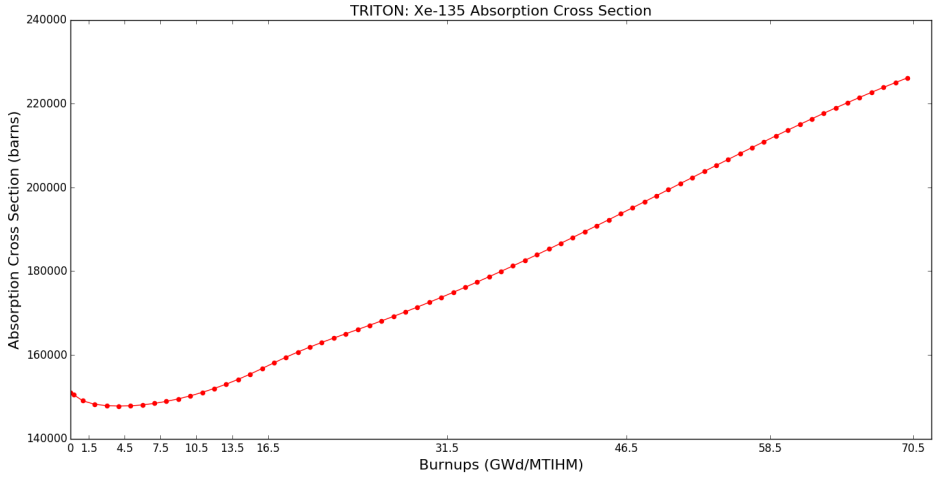

Figure 4: ^{135}Xe absorption cross section as a function of burnups in a GE 7x7-0 assembly.

In the comparisons, while the ^{135}Xe absorption cross section presents the greatest difference in absolute cross section difference, the relative percent difference remains below 1%. The next isotope with the greatest absolute difference is consistently the^{157}Gd absorption cross section; however, this one has a much greater relative percent difference as well. Figure 6 shows the one-group collapsed ^{157}Gd absorption cross section as a function of burnup as calculated by TRITON. The steep slope starting around 15 GWd/MTIHM corresponds to the burnups at which the greatest differences are observed in Figure 7. It is expected that rapidly changing cross sections such as this will be difficult to precisely approximate using interpolation.

Analysis then progressed on to the differences observed from linear interpolation over reactor parameter dimensions such as enrichment and moderator density. The results are much the same with the greatest differences observed in highly absorbing materials such as ^{155}Gd, ^{157}Gd, ^{149}Sm, and ^{135}Xe.

In general, the new Obiwan module for N-D library interpolation shows close agreement to the previous ARP methodology for burnup-dependent Origen reactor data interpolation. At present, due to computational cost considerations, Obiwan only provides a linear interpolation

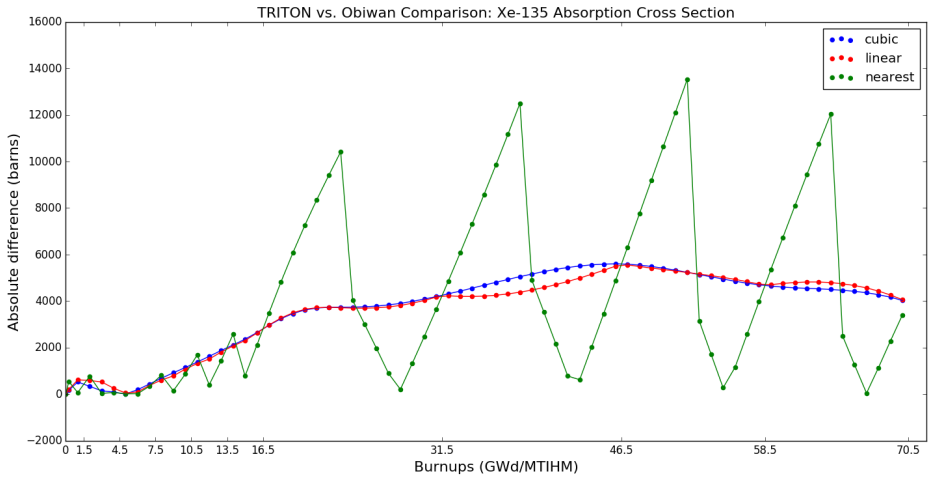

Figure 5: Absolute difference in the ^{135}Xe absorption cross section between TRITON and Obiwan as a function of burnups in a GE 7x7-0 assembly.

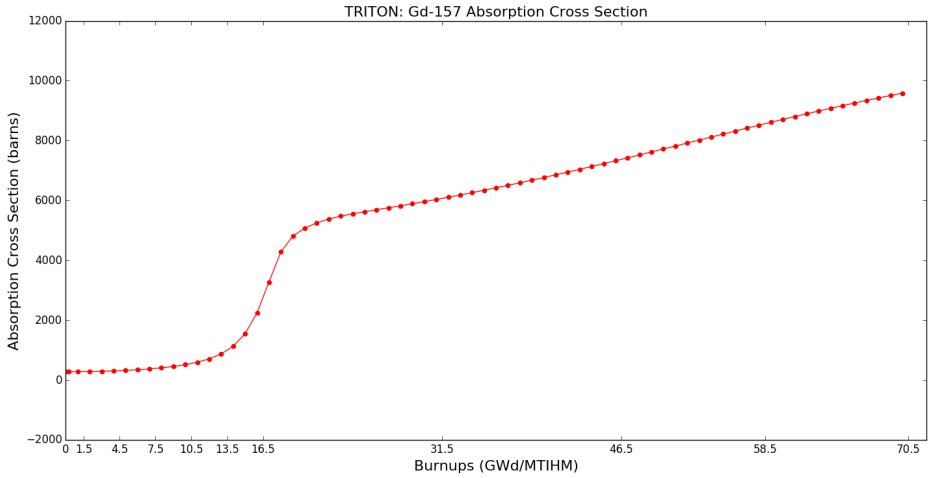

Figure 6: ^{157}Gd absorption cross section as a function of burnups in a GE 7x7-0 assembly.

implementation for generalized N-D interpolation over dimensions outside of burnup (e.g., enrichment, moderator density, etc.) While this method shows larger disparities compared to the lattice physics benchmark values (i.e., the interpolated values perform poorer especially for very strong neutron absorbers and for rapidly changing cross-sections), these differences still appear to be relatively small compared to the overall magnitude of the cross-sections in question.

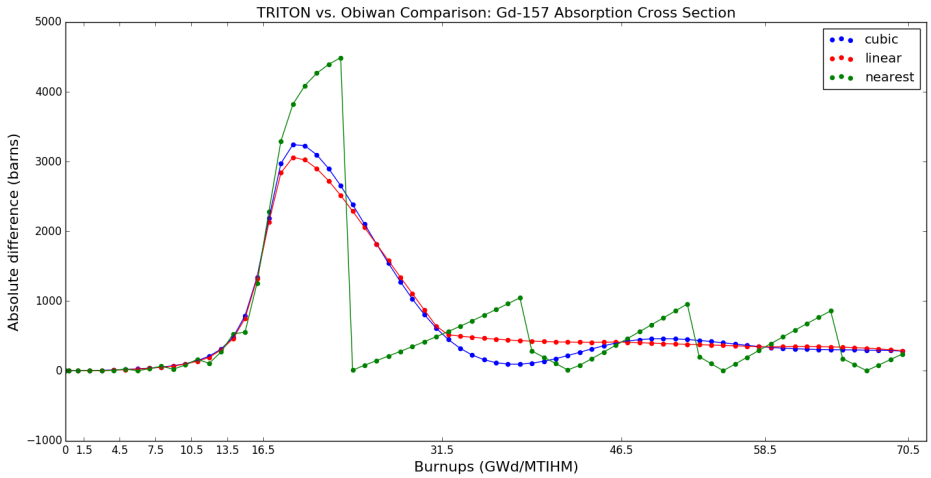

Figure 7: Absolute difference in the ^{157}Gd absorption cross section between TRITON and OBIWAN as a function of burnups in a GE 7x7-0 assembly.

2.1.5 Remaining development tasks

While generalized interpolation has now been implemented through the OBIWAN module (to be included in the upcoming SCALE 6.2 release), several desirable features still remain to be implemented. One such feature includes the development of a consolidated ORIGEN binary archive format, which would eliminate the need for separate on-disk library files for each library configuration permutation. Presently, each library configuration (e.g., unique combination of parameters such as burnup, moderator density, etc.) still resides in a separate on-disk file, albeit one that now provides descriptive information about the library within itself. When combined with methods we have developed to query all available on-disk ORIGEN library files within a directory, we have thus done away with the need for a separate, user-maintained text database listing of libraries (`arpdata.txt`). However, a fully portable solution will involve consolidation of individual library files into a master binary archive format for a larger grouping of libraries (e.g., all combinations of Westinghouse 17x17 assemblies). Development of this archive format has been moved down in terms of project priorities due to the closing of the SCALE 6.2 development window (given an anticipated public release later this year) as well as the need to expedite development toward more central project goals, such as the ORIGEN-based reactor module for CYCLUS. At present, sufficient generalized interpolation capabilities are now implemented to support this development, and thus it was decided to reallocate resources to archetype development tasks.

2.2 Validation of new CANDU PHWR assembly libraries for Origen

- **Targeted completion date:** March 2015
- **Task completion status:** 100%

During the last project period, a new set of CANDU PHWR fuel assembly lattices were developed for SCALE in order to generate new ORIGEN reactor data libraries for these fuel types based on modern nuclear data (illustrated as Figure 8). During the last project performance period, this work was successfully concluded.

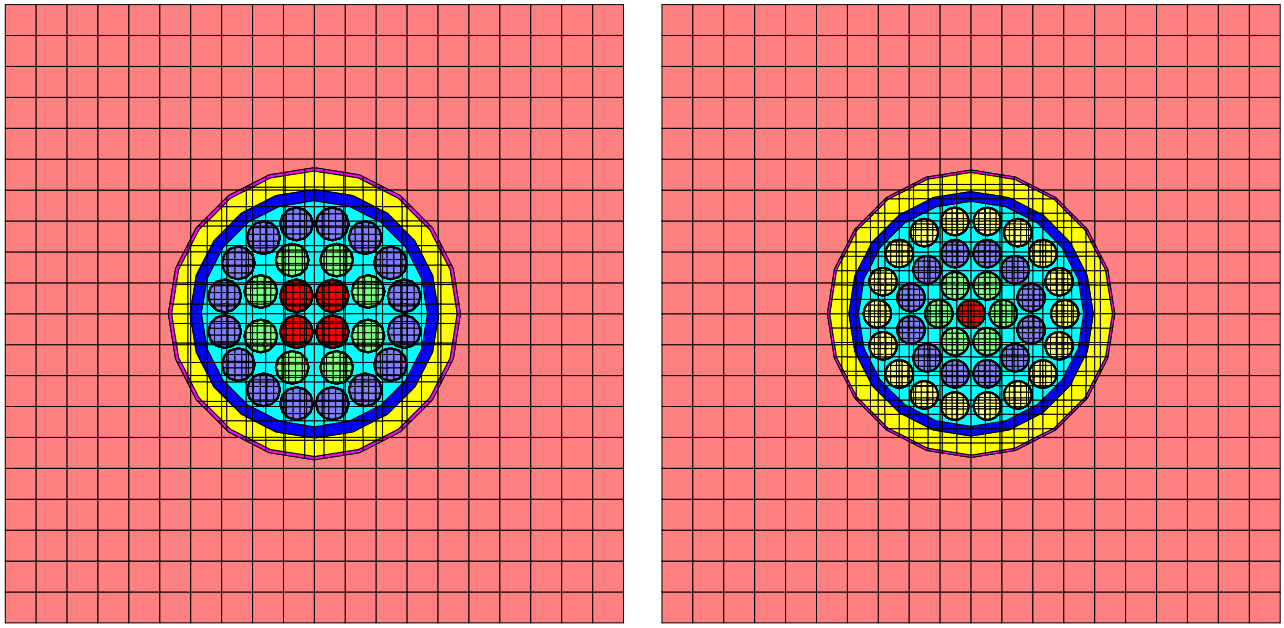

(a) CANDU 28-element bundle

(b) CANDU 37-element bundle

Figure 8: Final holes-based geometries for CANDU assembly lattices

A large component of the remaining work completed in the last performance period pertained to validation and benchmarking studies of the two lattices, the results of which were presented at the 2015 ANS Winter Meeting [20] and have been published as peer-reviewed journal article to *Nuclear Engineering and Design* [21].

This benchmarking effort sought to both characterize the performance of the SCALE lattices themselves (used to generate ORIGEN reactor data libraries) as well as the ORIGEN data libraries themselves.

2.2.1 CANDU lattice validation

This benchmarking consisted of both validation of the individual CANDU fuel assembly lattices (for the 28-element and 37-element designs). For the 28-element lattice, validation was performed by comparing the lattice performance against radiochemical assay data for both uranium and plutonium (Figure 9) as well as selected fission products and minor actinides (Figure 10). This benchmark compared the lattice performance for both older ENDF/V.2 data evaluations to ENDF/VII.0 to reported lattice benchmarks based on the prior lattice developed using WIMS-AECL, which was used as the basis for the prior ORIGEN library version. (It should be noted that no SCALE-compatible lattice existed for these fuel assembly designs previously). In addition, ENDF/VI.8 cross-sections were evaluated for minor actinides and fission products in order to confirm the potential effects of updated evaluations on ^{154}Eu and ^{155}Eu, after it was observed that even after extensive cross-checking of model parameters that these isotopes were calculated well outside of experimental uncertainty (discussed further in Section 2.3). Overall it was found that the new lattice using modern ENDF/VII.0 nuclear data performs well, calculating major actinide isotopes within experimental uncertainties and showing similar to improved agreement for nearly all benchmarked isotopes compared with the previous lattice with the notable exceptions of the Eu species.

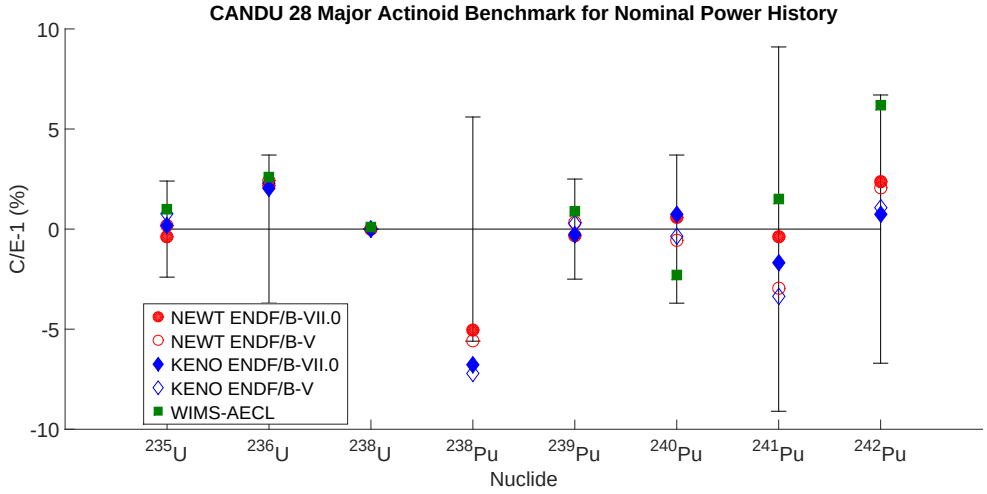

Figure 9: CANDU 28-element outer-ring depletion benchmark (based on Pickering-A outer-ring data using the nominal assembly power history) for major actinoids [10, 7]

The issue with matching Eu isotopic inventories would lead to the discovery of potential nuclear data discrepancies in the thermal neutron capture cross-sections of ^{154}Eu and ^{154}Sm. The discovery of this issue was directly tied to inherent features of the CANDU reactor design and its neutron energy spectra, however it is expected that these effects may have more modest but noticeable impacts for LWR fuel assembly calculations as well. Further details as to this investigation and

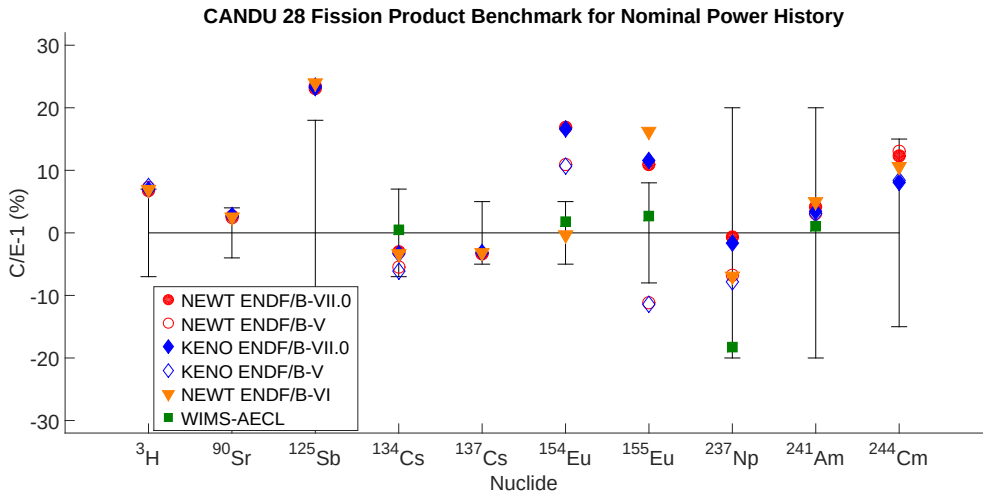

Figure 10: CANDU 28-element outer-ring depletion benchmark (based on Pickering-A outer-ring data using the nominal assembly power history) for fission products and minor actinoids [10, 7]

its findings are presented in Section 2.3.

In similar fashion to the 28-element lattice benchmarks, the 37-element lattice was also benchmarked; here, however, only data on uranium and plutonium species was available for comparison, presented as Figure 11. For this lattice benchmark, it was observed that the new lattice performs significantly better than the previously reported WIMS-based lattice for matching higher plutonium species (e.g., ^{241}Pu and ^{242}Pu); this was especially the case for studies employing the more recent ENDF/VII.0 evaluation (which contains significantly more resonance capture information).

Overall the lattice benchmarks appear to indicate superior performance of the new lattices compared to the prior published benchmark.

2.2.2 Origen reactor data library validation for CANDU libraries

With the validation of the lattice templates used to generate ORIGEN reactor data libraries, the next step was to validate the performance of the ORIGEN libraries themselves generated from the templates. While similar to the previous process, this validation introduces particular complications for the validation of the 28-element assembly, given that the benchmark data for this assembly is for a single outer-ring fuel element, whereas the ORIGEN reactor data library represents an assembly-averaged flux spectra. In as much, the shape of the flux spectra for this library does not truly reflect that of the benchmark data; however, given the absence of other benchmark data, we made the decision to proceed with a modified benchmark based on adjusting the inferred outer element power history to better match the depletion of ^{235}U (thereby matching

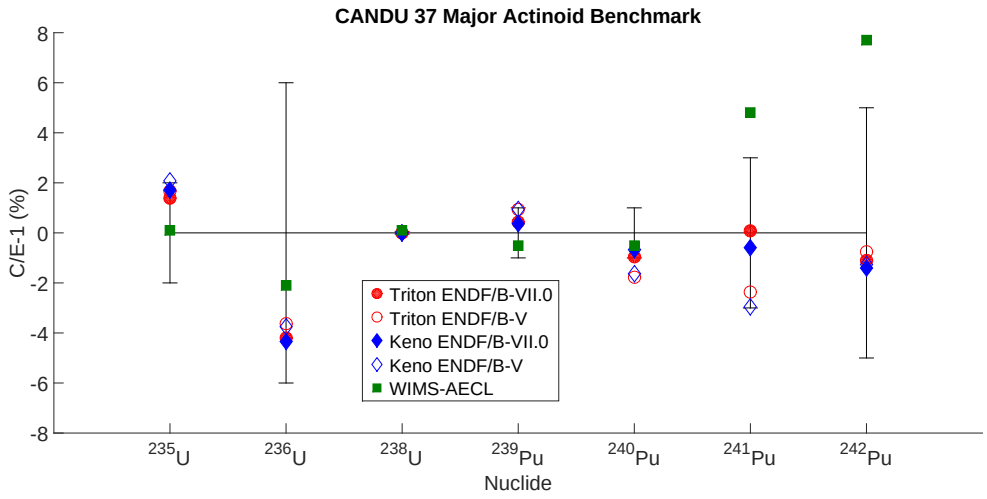

Figure 11: CANDU 37-element bundle depletion benchmark (based on Bruce-A assembly data) for major actinoids [10, 7].

the element's discharge burnup value). This benchmark is presented for major actinoids and selected fission products with minor actinoids as Figures 12 and 13, respectively.

Within these benchmarks, an additional test is provided involving the use of a modified AMPX master multi-group library reflecting ENDF/VI.8 thermal neutron capture cross-sections (denoted as the "modified" library). Overall the new ORIGEN library for the 28-element lattice shows similar to improved agreement for most uranium and plutonium species, with the exception of ^{242}Pu, for which both the old and new library calculated as outside the experimental uncertainty. This is likely due to the fact that the production of higher actinoid species (such as both ^{242}Pu and ^{244}Cm) is highly dependent upon the shape of the neutron energy spectrum; in as much, a mismatch here would likely be reflected in the calculated inventories as well. (Such a mismatch would be due to the fact than assembly-averaged spectrum is applied to a benchmark for a single pin, as discussed previously.) For the fission products, the new library performs approximately similar to the previous ORIGEN library, with a few notable exceptions including ^{125}Sb and ^{155}Eu. It should be noted that the correction introduced to the ^{154}Eu thermal capture cross-section drives up inventories of ^{155}Eu, thereby further over-predicting this species; further investigation of this phenomenon is presented in the following section. With respect to the minor actinoid species, the new library overall performs similarly to the previous version, with the exception of ^{244}Cm, wherein the new library further over-predicts ^{244}Cm inventories by a substantial margin; however, it should be noted that neither the old nor the new library correctly calculates this isotope within experimental uncertainties, again potentially indicating a problem with the benchmark itself.

For the 37-element library, the benchmark is comparatively more straightforward (shown as Figure 14). Because the benchmark for this case was for an entire dissolved assembly, the ORIGEN benchmark corresponds much more closely to the actual radiochemical data used. Both libraries

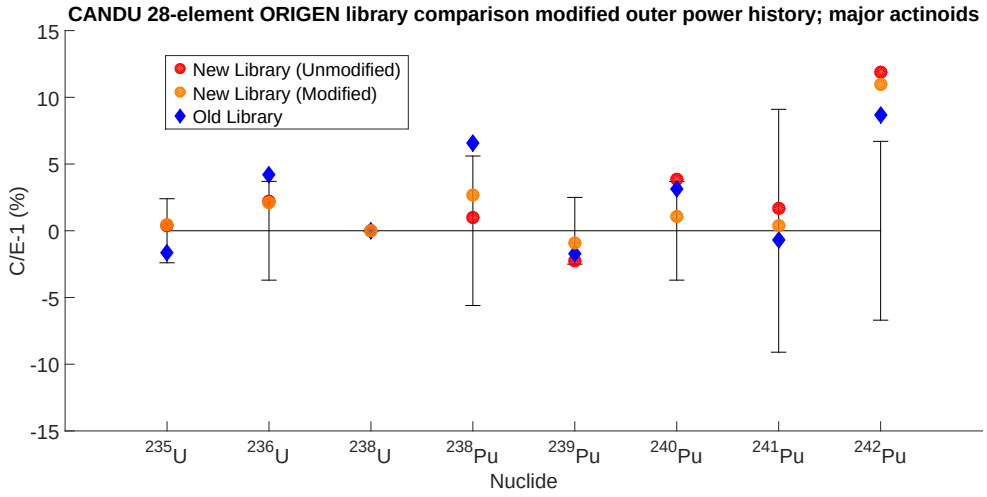

Figure 12: CANDU 28-element ORIGEN library comparison modified outer element power history; major actinoids. Note that benchmark inventories are rescaled from edge element values (per [7]) to produce an assembly-averaged value.

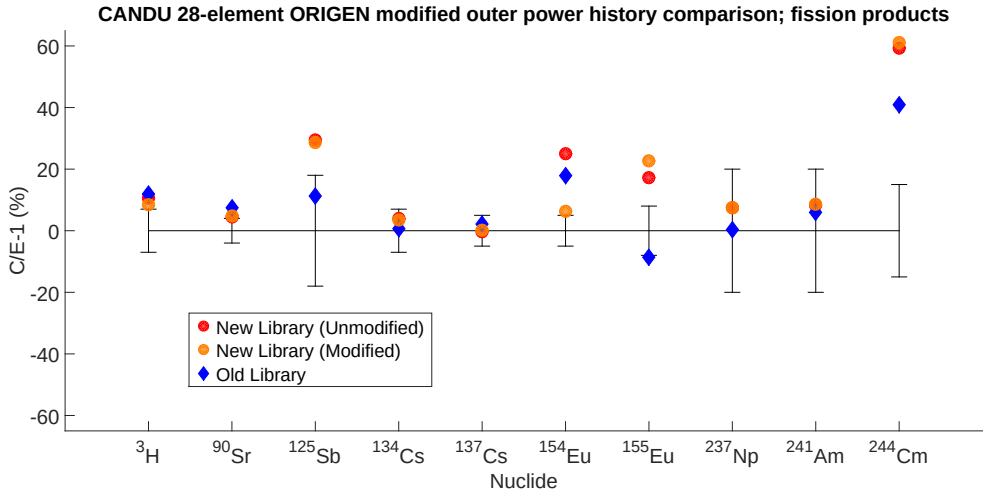

Figure 13: CANDU 28-element ORIGEN library comparison modified outer element power history; fission products and minor actinoids

give calculated inventories for U and Pu isotopes well within experimental uncertainties, with the new library giving values that generally show slightly improved agreement to benchmark values (although these differences are not significant).

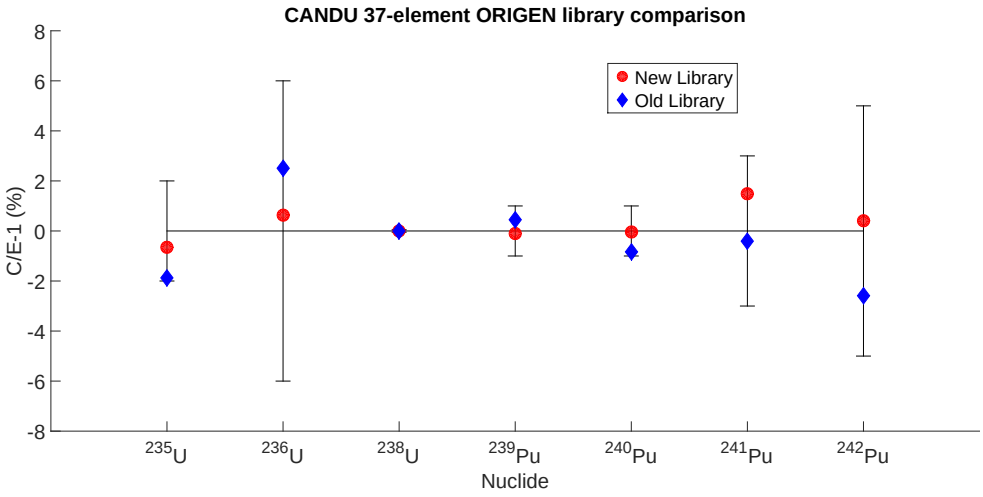

Figure 14: CANDU 37-element ORIGEN library comparison

2.3 Discovery of potential nuclear data discrepancies: Eu-154

- **Targeted completion date:** N/A
- **Task completion status:** Completed

The previous WIMS-based 28-element library was able to achieve reasonable prediction of ^{154}Eu and ^{155}Eu by using ENDF/B-VI cross-sections for these isotopes. The ENDF/B-VI.8 library did produce accurate inventory predictions for ^{154}Eu (with a difference of about 1.34%, well within experimental uncertainty), however ^{155}Eu was still predicted higher than the experimental value by about 15%. One plausible explanation for this deviation is due to the evaluated radiative capture cross-sections for Eu species in the thermal region, and in particular the differences in evaluated capture cross-section values between ENDF/B-V.2, VI.8, and VII.0. The ENDF/B-VI.8 cross-sections for ^{154}Eu produced good agreement for ^{154}Eu, however, ^{155}Eu was not produced within the measurement uncertainty bounds for any cross-section library.

To understand this issue, it is first important to understand the production and loss channels for Eu species, which can be represented by the general expression in Equation 2.

$$\frac{dN_i}{dt} = \overbrace{\sum_{m=1}^{M} Y_m \lambda_m N_m}^{\text{A}} + \underbrace{\phi \sigma_{i-1}^a N_{i-1}}_{\text{B}} - \overbrace{\lambda_i N_i}^{\text{C}} - \underbrace{\phi \sigma_i^a N_i}_{\text{D}} + \overbrace{Y_i \Sigma_f \phi}^{\text{E}} + \underbrace{\sum_{m \neq i} N_m \sigma_{m \to i} \phi}_{\text{F}} \tag{2}$$

where

- Term A = Production of nuclide i from M parent isotope decays
- Term B = Production of nuclide i from neutron absorption
- Term C = Loss of nuclide i to decay
- Term D = Loss of nuclide i to neutron absorption
- Term E = Direct production of nuclide i from fission
- Term F = Other neutron-induced reactions (e.g., (n,p), (n,2n), etc.)

The dominant terms controlling the ^{154}Eu and ^{155}Eu inventories are (A), (B), and (D). Given that the direct fission yields of ^{154}Eu and ^{155}Eu from ^{235}U and ^{239}Pu are both vanishingly small, the predominant production channels for both species are therefore through parent isotope decays (e.g., for ^{155}Eu from the decay of ^{155}Sm) as well as through successive neutron capture reactions, i.e. $^{153}\text{Eu}\,(\text{n},\gamma)^{154}\text{Eu}$ and $^{154}\text{Eu}\,(\text{n},\gamma)^{155}\text{Eu}$. ^{153}Eu, ^{154}Eu, and ^{155}Eu all have relatively high thermal-region neutron capture cross-sections, ranging from about 335 barns for ^{153}Eu [2] to several thousand barns for ^{154}Eu and ^{155}Eu (with even higher capture cross-sections in the resonance energy regions), making capture a predominant production and loss channel for these species.

To understand the relative contributions to nuclide production and loss, it is helpful to refer to the ORIGEN transition matrix $\overline{\overline{A}}$, which describes the total transition rate constant for each set of coupled differential equations describing the system, i.e. [11]:

$$\frac{d\overline{N}}{dt} = \overline{\overline{A}} \cdot \overline{N}\,(t) \tag{3}$$

The transition matrix $\overline{\overline{A}}$ describes the transition rate coefficients for each isotopic transition from neutron reactions and decay. Thus, each individual element of $\overline{\overline{A}}$ (denoted a_{ij}) describes the relative transition rate from nuclide i to j [11]:

$$a_{ij} = -\ell_{ij}\lambda_i - f_{ij}\overline{\phi}\sigma_i \tag{4}$$

Where ℓ_{ij} is the decay yield from nuclide i to nuclide j and f_{ij} is the reaction yield, $\overline{\phi}$ is the collapsed one-group flux, and σ_i is the one-group flux-weighted reaction cross-section. Thus,

individual transition coefficients can be thought of as relative indicators of the rates of production and loss into individual nuclides. Evaluated this way, it is evident in Tables 1 and 2 (which list the most significant gain and loss transition coefficients for ^{154}Eu and ^{155}Eu) that neutron capture is by far the dominant gain and loss channel for both species.

Table 1: Reaction-based gain and loss channels for ^{154}Eu, based on the ORIGEN transition matrix for a CANDU 28-element assembly at the start of irradiation (0 $\frac{\text{MWd}}{\text{MTU}}$). (Note that only the 5 most significant transitions are given.)

^{154}Eu gains		^{154}Eu losses	
Reaction	a_{ij}	Reaction	a_{ij}
$^{153}\text{Eu}\,(n,\gamma)\,^{154}\text{Eu}$	1.1038E+02	$^{154}\text{Eu}\,(n,\gamma)\,^{155}\text{Eu}$	6.6322E+02
$^{249}\text{Cf}\,(n,f)\,^{154}\text{Eu}$	3.5425E-03	$^{154}\text{Eu}\,(n,n)\,^{154\text{m}}\text{Eu}$	5.5964E-02
$^{243}\text{Cm}\,(n,f)\,^{154}\text{Eu}$	7.0951E-04	$^{154}\text{Eu}\,(n,2n)\,^{153}\text{Eu}$	2.1322E-03
$^{242}\text{Am}\,(n,f)\,^{154}\text{Eu}$	6.3834E-04	$^{154}\text{Eu}\,(n,p)\,^{154}\text{Sm}$	6.1756E-06
$^{251}\text{Cf}\,(n,f)\,^{154}\text{Eu}$	3.6207E-04	$^{154}\text{Eu}\,(n,\alpha)\,^{150}\text{Pm}$	4.3990E-08

Table 2: Reaction-based gain and loss channels for ^{155}Eu, based on the ORIGEN transition matrix for a CANDU 28-element assembly at the start of irradiation (0 $\frac{\text{MWd}}{\text{MTU}}$). (Note that only the 5 most significant transitions are given.)

^{155}Eu gains		^{155}Eu losses	
Reaction	a_{ij}	Reaction	a_{ij}
$^{154}\text{Eu}\,(n,\gamma)\,^{155}\text{Eu}$	6.6322E+02	$^{155}\text{Eu}\,(n,\gamma)\,^{156}\text{Eu}$	1.4438E+03
$^{249}\text{Cf}\,(n,f)\,^{155}\text{Eu}$	4.2343E-02	$^{155}\text{Eu}\,(n,2n)\,^{154}\text{Eu}$	3.0927E-04
$^{242}\text{Am}\,(n,f)\,^{155}\text{Eu}$	1.0235E-02	$^{155}\text{Eu}\,(n,2n)\,^{154\text{m}}\text{Eu}$	1.2106E-04
$^{243}\text{Cm}\,(n,f)\,^{155}\text{Eu}$	9.5522E-03	$^{155}\text{Eu}\,(n,p)\,^{155}\text{Sm}$	3.5362E-06
$^{251}\text{Cf}\,(n,f)\,^{155}\text{Eu}$	7.1689E-03	$^{155}\text{Eu}\,(n,\alpha)\,^{152\text{m}}\text{Pm}$	1.6364E-06

Particularly useful in understanding the miscalculations of Eu species is a comparison of the thermal-region capture cross-sections for ^{153}Eu and ^{154}Eu, shown in Figure 15. Here, the $^{153}\text{Eu}(n,\gamma)^{154}\text{Eu}$ cross-section is consistent between ENDF/B-VI.8 and ENDF/B-VII.0 [3, 5]. However the ENDF/B-VII.1 evaluation reports a discrepancy of approximately 11% found with experimental values [4]; thus the 2200 m/s thermal cross-section was corrected from 312 b to 358 bn in the newest evaluation, consistent with what is seen in Figure 15(b). However, given the consistency between ENDF-VI.8 and ENDF-VII.0, this can be ruled out as the source of the discrepancy in ^{154}Eu inventories.

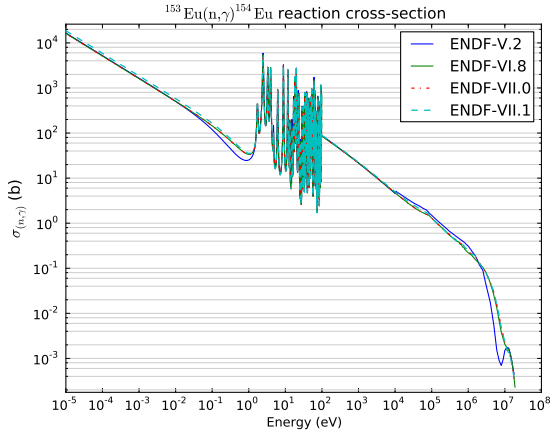

(a) ^{153}Eu(n,γ)^{154}Eu cross-section

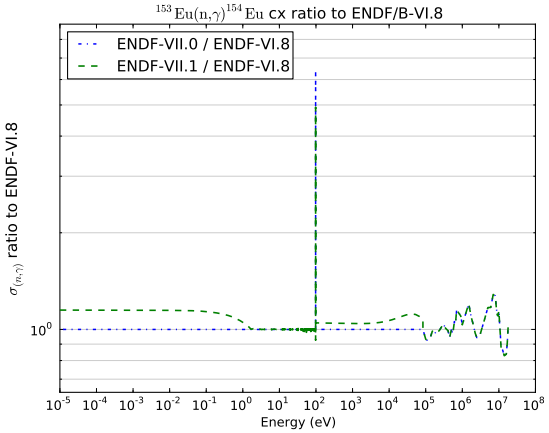

(b) ^{153}Eu(n,γ)^{154}Eu cross-section ratios

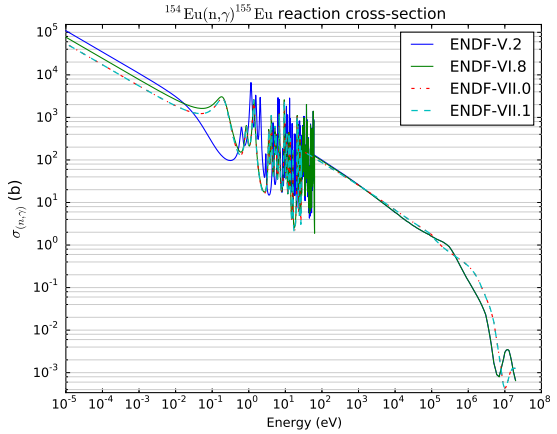

(c) ^{154}Eu(n,γ)^{155}Eu cross-section

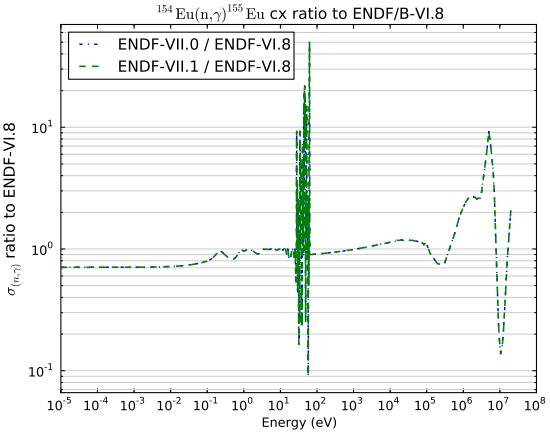

(d) ^{154}Eu(n,γ)^{155}Eu cross-section ratios

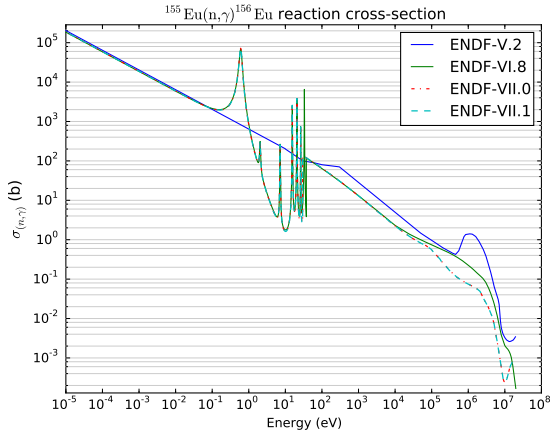

(e) ^{155}Eu(n,γ)^{156}Eu cross-section

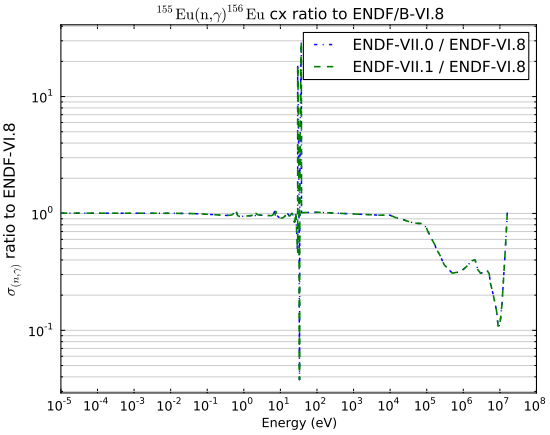

(f) ^{155}Eu(n,γ)^{156}Eu cross-section ratios

Figure 15: Radiative capture (n,γ) cross-sections for several ENDF library evaluations (left) and capture cross-section ratios to ENDF-VI.8 data (right) for ^{153}Eu,^{154}Eu, and ^{155}Eu. [3, 5]

Likely at cause for the over-prediction is the ^{154}Eu$(n,\gamma)^{155}$Eu capture cross-section, which is approximately 40% lower for the 2200 m/s evaluation for ENDF-VII.0 compared to ENDF-VI.8. The 0.0254 eV cross-section in ENDF/B-VI.8 is based on evaluations by Sekine et. al., indicating a value of 1840 barns for the radiative capture cross-section [19]. The evaluation used in ENDF/B-VII.0 cites Mughabghab for an evaluated thermal capture cross-section of 1348.5 barns [17], however no mention is made of the prior evaluation by Sekine et. al. [19]. Further, File 2 (MF=2) of the ENDF/B-VII.0 library gives a calculated thermal capture cross-section of 1841.6 barns [3], which is 36.6% higher than the evaluated value and consistent with Sekine [19]. Thus, given this and the better observed agreement seen for ^{154}Eu when using the ENDF/B-VI.8 library, it appears likely that the ENDF/B-VII.0 and VII.1 libraries are in error for the ^{154}Eu thermal capture cross-section, which would thus explain the observed discrepancy.

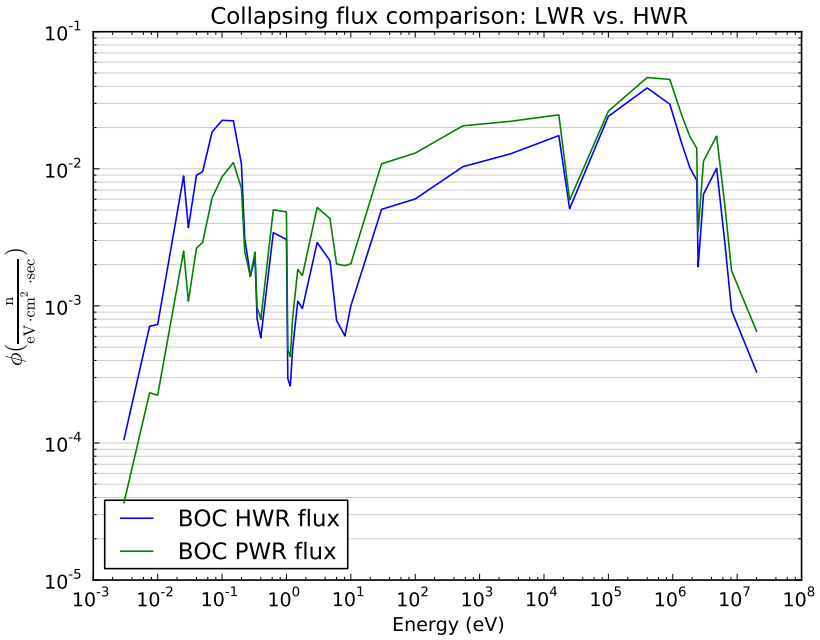

Figure 16: Distribution of the 49-group collapsing flux used at the beginning-of-core for a typical PWR assembly (Westinghouse 17x17) versus a CANDU PHWR (28-element) assembly. Note the shift of the neutron population away from the resonance region and toward the thermal region for heavy-water spectra compared to a corresponding light-water reactor spectrum.

Further compounding this issue is the fact that the highly-thermalized neutron energy spectrum for heavy-water moderators heightens the sensitivity to these cross-section differences compared with light-water spectra, as seen by the representative beginning-of-core assembly-average flux profile shown in Figure 16. Here, the average thermal-region neutron population for a HWR

is nearly double that of a typical LWR (calculated for a Westinghouse 17x17 PWR assembly). Thus, the heavy-water lattice models are arguably more sensitive to the observed differences in the thermal-region absorption cross-sections (while being subsequently less sensitive to changes in the resonance region).

Meanwhile, ^{155}Eu is not accurately predicted by any of the libraries. Here, the production is too high for ENDF-B/V and too low for ENDF/B-VII.0. Looking at the production of ^{155}Eu via the neutron absorption from the $^{154}\mathrm{Eu}(n,\gamma)^{155}\mathrm{Eu}$ reaction does not appear to immediately explain the discrepancy. ENDF/B-V.2 contains no resonance information; the cross-section is interpolated through the resonance region, likely explaining the over-prediction for ENDF-V libraries. Conversely, the ENDF/B-VII.0 evaluation reports a thermal capture cross-section of 3,758.4 barns, with a resonance integral of 15,527.5 barns [3]; identical values are reported for ENDF/B-VII.1 [4]. The ENDF/B-VI.8 evaluation reports a thermal capture cross-section of 3,760.22 barns with a resonance integral of 15,288 barns [5].

Given the similarities between the ENDF-VI.8 and VII.0 evaluations, it appears unlikely that the $^{155}\mathrm{Eu(n,}\gamma)^{156}$Eu cross-section is at issue, but rather that there may be other production channels at issue (i.e., neutron capture by ^{154}Sm, the dominant loss channel with a transition coefficient of 3.3521 s^{-1}, drives β^- decay by ^{155}Sm into ^{155}Eu). This hypothesis is further supported by the differences in the evaluation of the $^{154}\mathrm{Sm}(n,\gamma)^{155}\mathrm{Sm}$ reaction between ENDF/B-VI.2 and ENDF/B-VII.0 and VII.1, wherein the thermal capture cross-section for the latter evaluations are approximately 10% higher than the ENDF/B-VI.2 evaluation, thus driving a larger decay source term by ^{155}Sm into ^{155}Eu.

2.4 Prior observed discrepancies in ^{154}Eu in used fuel benchmark studies

Upon further investigation, it was observed that discrepancies in the CANDU 28-element assembly were not an isolated phenomena but simply a more extreme outlier in a common trend in over-predictions of ^{154}Eu inventories across a number of spent fuel benchmarking studies. Table 3 illustrates this for several published benchmarks of used fuel assemblies based on destructive chemical assay data, where one will observe for light water reactor assemblies typical over-estimations of the ^{154}Eu inventory range from about 7–13% for ENDF/B-VII.0 and 9–14% for ENDF/B-VII.1.

This lead to further questions as to potential changes that may have occurred to the ^{154}Eu cross-section evaluation between different nuclear data releases and the potential effects on calculated inventories, each of which is explored in the following sections.

2.5 ^{153}Eu & ^{154}Eu radiative capture cross-section evaluations

Figures 15(a) and 15(c) illustrate the radiative capture cross-sections for ^{153}Eu and ^{154}Eu across different nuclear data evaluations. With the exception of the transition from ENDF/B-VII.0 to VII.1 (wherein there is a 15% upward adjustment in the $^{153}\mathrm{Eu}\,(\mathrm{n},\gamma)\,^{154}$Eu thermal capture

Table 3: Calculated to experiment (C/E) ratios for ^{154}Eu from recent spent fuel benchmarking studies using ENDF/B-VII.0 and VII.1 data; ENDF/B-VII.0 and VII.1 C/E data adapted from evaluations in [23] with original benchmarking studies indicated.

Assembly / Sample	Type	# samples	$\overline{\sigma}$	Average C/E	
				ENDF-VII.0	ENDF-VII.1
TMI-1 NJ05YU [9]	B&W 15×15	5	0.021	1.1151	1.1311
Calvert Cliffs MKP-109 [14]	CE 14×14	3	0.074	1.0647	1.0924
REBUS GKN-II [15]	18×18	1	0.017	1.1320	1.1448
ARIANE GU1 [15]	15×15	1	0.020	1.1283	1.1391
Vandellós II [13]	West. 17×17	3	0.104	1.0971	1.1209
Pickering-A 19558C [21]	CANDU-28	1	0.050	1.1623	1.2641

cross-section due to new experimental data incorporated into the evaluation), the ^{153}Eu radiative capture cross-section is effectively unchanged between evaluations. Thus, while enhanced capture by ^{153}Eu in the ENDF/B-VII.1 evaluation would explain a small component of overestimates of ^{154}Eu, this alone is insufficient to explain the observed bias.

Meanwhile, one will observe that between the ENDF/B-VI.8 and VII.0 evaluations, there is a far more dramatic change to the thermal-region capture cross-section, wherein the thermal capture cross-section in ENDF/B-VI.8 (evaluated by R.Q. Wright of ORNL) of 1840 barns is based on measurements conducted by Sekine et. al. [19]; ENDF/B-VII.0 reports a value of 1340 ± 130 barns calculated by Mughabghab [17], a 36.6% difference. This significant change in the absorption cross-section would easily explain the over-estimations in the ^{154}Eu inventories observed, namely by suppressing the thermal capture rate by ^{154}Eu.

Mughabghab points out that the 1840 barn thermal capture cross-section reported by Sekine et. al. assumes a $1/v$ Wescott factor of unity, whereas the correct value would be $g_w = 1.237$ [23]; thus, the true thermal capture cross-section (rather than the Maxwellian-weighted value) would be around 1488 ± 73 barns [23]. For comparison, historical evaluated values of the 2200 $^{m}/_{s}$ cross-section are reported in Table 4; here, one will observe that the corrected Sekine value lies just over the 1-σ uncertainty bounds from the original value reported by Mughabghab [17]. This Wescott-corrected value will serve as a basis of comparison for proposed revisions to the cross-section value discussed in the next section.

2.5.1 Evaluated modifications to the ^{154}Eu radiative capture cross-section

Based on the differences in the ENDF/B-VI.8 evaluation (performed by R. Q. Wright) and ENDF/B-VII.0, one amendment to the ^{154}Eu thermal capture cross-section that could be inferred would be to restore the resolved resonance treatments evaluated by Wright, including a bound state at -0.71 eV and adjusting the first resolved resonance at 0.190 eV (hereafter referred to

Table 4: Measured and evaluated 2200 $^{m}/_{s}$ capture cross-sections (σ_{th}) for ^{154}Eu

Evaluator	Type	σ_{th} (bn)	Uncert. (bn)
Hayden et. al. [12]	Exp.	880	—
Vertebnyj et. al. [24]	Exp.	1250	160
Sekine et. al. [19]	Exp.	1840	90
Mughabghab [17]	Calc.	1340	130

as the "Wright" evaluation). An alternative evaluation, proposed by Mughabghab, would be to shift the location of the first resolved resonance from 0.195 eV to 0.188 eV based on results reported by Anufriev [1]; this in turn would also incorporate adjusting the neutron width (Γ_n) proportional to $\frac{1}{\sqrt{E}}$, i.e. by a factor of $\sqrt{\frac{0.195}{0.188}} = 1.018$ (referred to hereafter as "Mughabghab"). The modifications ot the ENDF resolved resonance evaluations for each of these evaluations is explicitly shown as Table 5.

Table 5: Evaluated modifications to the ENDF/VII.0 / VII.1 $^{154}\mathrm{Eu}\,(\mathrm{n},\gamma)^{155}$ Eu resolved resonance parameters, based on the ENDF/B-VI.8 thermal-region behavior ("Wright") and changes proposed by Mughabghab ("Mughabghab"). Note that the changes based on ENDF/B-VI.8 ("Wright") introduces an additional bound state at -0.71 eV not present in the VII.0 or VII.1 evaluations.

Evaluation	E (eV)	$\lvert J\rvert$	Γ	Γ_n	Γ_γ
Wright	-0.7100000	2.5	0.1264160	4.160000E-4	0.1260000
	0.1900000	3.5	0.1600595	5.950000E-5	0.1600000
Mughabghab	0.1880000	2.5	0.1500731	7.307365E-5	0.1500000

Applying each of the two proposed modifications in Table 5 to the ENDF/B-VII.0 and VII.1 resolved resonances for ^{154}Eu, new AMPX master continuous energy (CE) libraries were developed for use with the TRITON/NEWT discrete ordinates transport sequence to evaluate the effect of modifying the thermal capture resolved resonance parameters. While TRITON/NEWT makes use of multi-group nuclear data in its lattice physics treatment, the CENTRM module used to process resonance self-shielding uses AMPX CE data to update the multigroup libraries; thus, updating the AMPX CE data used by TRITON was required to perform this evaluation. This updated CE data is then propagated by CENTRM into the calculation to produce updated multi-group libraries used in the lattice physics calculation.

The updated pointwise cross-sections for the thermal resonance region are shown in Figure 17. Here, the primary difference between the evaluations is in the centroid and intensity of the first resolved resonance and likewise the $^{1}/_{v}$ thermal region of the cross-section.

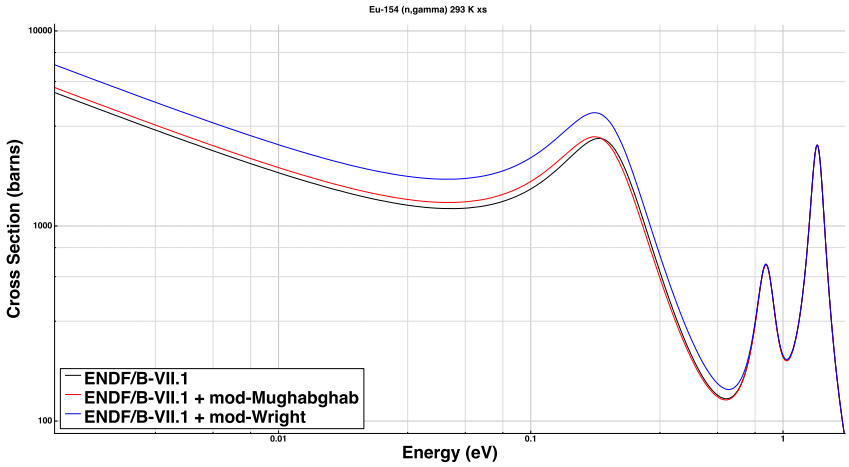

Figure 17: Original ENDF/B-VII.0 & VII.1 treatment for the thermal region of the $^{154}\mathrm{Eu}\,(\mathrm{n},\gamma)\,^{155}\mathrm{Eu}$ cross-section, along treatments based on restoring the ENDF/B-VI.8 bound state and first resolved resonance ("Wright") and by shifting the location of the first resolved resonance and adjusting the neutron width proportionally ("Mughabghab").

Note that previously-conducted integral benchmark evaluations using the Wright treatment appear to overestimate ^{154}Eu captures, leading to underestimation of the ^{154}Eu inventory in most samples evaluated [23]. Conversely, the Mughabghab treatment shows consistently improved agreement with experimental values for both ENDF/B-VII.0 and VII.1 although still producing noticable overestimates of ^{154}Eu inventories for most cases [23]. As a result, this analysis will focus exclusively upon the modifications to the ^{154}Eu thermal capture evaluation proposed by Mughabghab.

2.5.2 Integral benchmarking with the updated Eu-154 cross-section

The evaluation of the ^{154}Eu thermal capture cross-section culminated in the identification of a potential adjustment to the first resolved resonance (at around 0.1 eV). Following on this work, a series of benchmarks was performed on several known spent fuel assays (i.e., reproducing the studies in Table 3 with a modified cross-section library) to demonstrate the effect of the updated evaluation, summarized as Figure 19.

In particular, one will observe from Figure 19 that the proposed modification to the ^{154}Eu capture cross-section produces an overall superior agreement to spent fuel benchmarks over a wide range of fuel burnups, indicating that the targeted region may indeed be contributing to over-estimation of ^{154}Eu by underestimating the rate of capture into ^{155}Eu.

This evaluation work has been presented and published at two conferences, including the PHYSOR 2016 conference and the M&C 2017 conference, as well as being published as a peer-

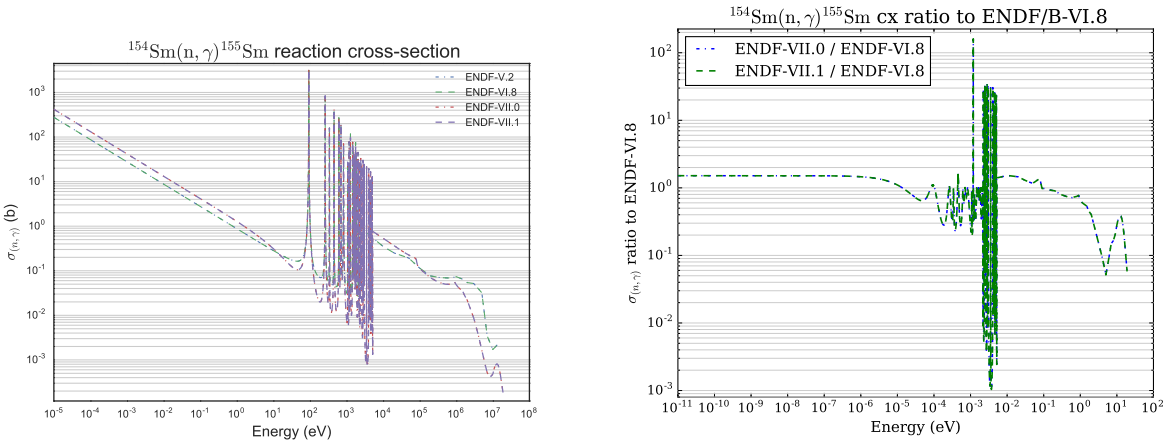

(a) ^{154}Sm(n,γ)^{155}Sm cross-section (b) ^{154}Sm(n,γ)^{155}Sm cross-section ratios

Figure 18: Radiative capture (n,γ) cross-sections for several ENDF library evaluations (left) and capture cross-section ratios to ENDF-VI.8 data (right) for ^{154}Sm. [3, 5]

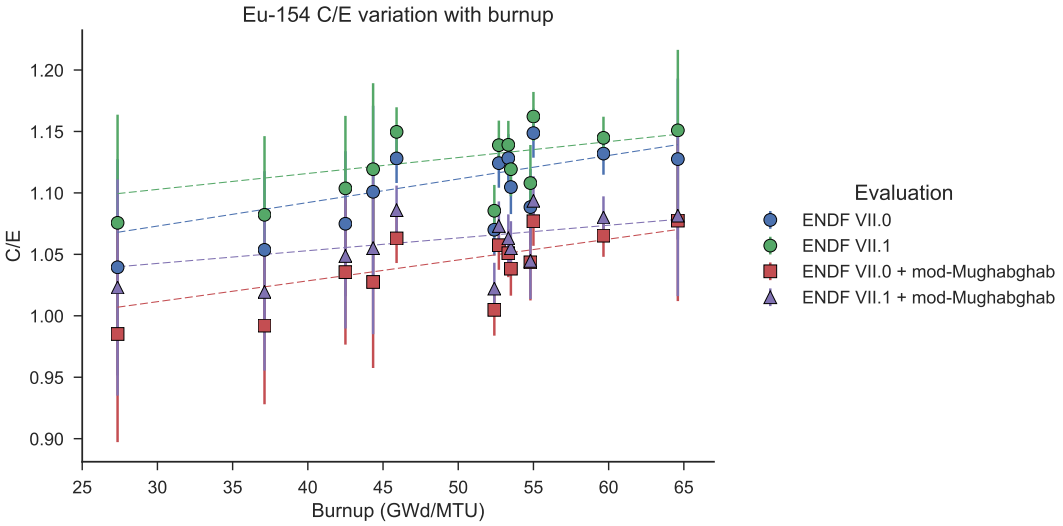

Figure 19: C/E values for ^{154}Eu for all PWR-based fuel benchmarks and evaluations considered (i.e., all benchmarks save for the CANDU 28-element assembly), evaluated as a function of sample burnup. One will observe that discrepancies in the predicted ^{154}Eu follow a linear trend with burnup, especially for the original ENDF/B-VII.0 and VII.1 evaluations.

reviewed journal publication [23]. The results have likewise been communicated to the Cross Section Evaluation Working Group (CSEWG) and has also contributed to new proposed research at ORNL to experimentally re-measure the ^{154}Eu neutron capture cross-section in this energy region.

2.6 Validation studies of unmodified PWR lattice templates

- **Targeted completion date:** March 2015
- **Task completion status:** 100%

In the original project plan, we had proposed development of modernized reactor data libraries for ORIGEN. However, between the time of proposal and award, separate parallel work was already being undertaken by researcher at ORNL on this task to modernize and test the existing reactor data library templates for LWR assembly types. Thus, this project component evolved toward the end of validating the performance of unmodified SCALE reactor data lattice templates for PWR assemblies in their "unmodified" state; i.e., without consideration of features such as the presence of burnable poisons, soluble boron, and other features which would not be captured in the typical use case within ORIGEN. Here, the goal of this study was to characterize the typical level of accuracy that could be expected using unmodified ORIGEN templates (in the context of on-disk, interpolated library files) to represent specific fuel conditions.

The approach taken for this study likewise incorporated novel use of multivariate analysis to understand the major contributors to the variance in isotopic inventories, i.e. how much of the variation in isotopic inventories could be attributed directly to gross features such as discharge burnup, thereby quantifying the envelope of variation in isotopic inventories due to assembly-specific features not typically captured in ORIGEN calculations (such as the presence of burnable poisons, soluble boron levels, etc.).

An additional aim of this analysis is to evaluate the accuracy of using assembly-averaged models to estimate the isotopic content of specific fuel pins. Because ORIGEN cross-section libraries use the assembly-averaged collapsed one-group spectrum, these data libraries therefore inherently represent an assembly-averaged flux. While a more accurate approach to evaluating pin-specific properties would be to model the full assembly and deplete pins of interest separately, here the goal is to convey how well an assembly-averaged model (such as those represented by the ORIGEN reactor data libraries) can capture specific pin features measured in prior radiochemical assay studies.

For the purposes of this study, SCALE 6.1 was used to carry out depletion calculations which were compared against experimental assays. This report examines fuel samples from a variety of programs with a wide range of burnups. Except where noted, the geometry of the templates was held constant; only the interpolable template parameters (e.g., enrichment, cycle power, cycle length, and inter-cycle decay time) were modified.

In addition to benchmarking several unmodified PWR lattices, this study examined the use of multivariate analysis techniques to analyze trends in the isotopics, including principal component analysis (PCA) and partial least squares regressions (PLS). PCA is used to compare the linear relationships in large sets of data. For this analysis, PCA is used help visualize and compare the calculated isotopics to the experimental assay values.

PLS is used to determine which parameters are important for lattice physics calculation, how much of the isotopic variance can be explained by particular parameters such as burnup. This study primary focused on the lattice performance without modeling of more advanced parameters such as the boron letdown curve or proximity to burnable absorbers. It is important to note that PLS can only capture linear variance; thus, non-linear variances cannot be accounted for. Initial results show that 85% of the variance in the measured major actinides can be explained by the variance in the burnup.

2.6.1 Validation of unmodified SCALE PWR templates

Four PWR lattices were studied for this work, based on the availability of radiochemical assay benchmarks: Babcock and Wilcox 15x15, Westinghouse 15x15, and Westinghouse 17x17. Each template was run only changing the default parameters for enrichment and assembly power. The templates were evaluated using the 238-group AMPX master library based on ENDF/VII.0 data in Triton.

In order to more effectively analyze trends in evaluated assembly isotopic values compared to benchmark data, plots are given for select major and minor actinides. The selected actinides were the most commonly collected data cross the different assay studies. The plots aim to analyze trends in these isotopes across burnup for a particular assembly. Frequently, rapid depletion or simplified lattice physics models are run to determine spent fuel plutonium content. For this reason, this analysis focuses on the plutonium inventories calculated by these unmodified templates.

The Westinghouse 15x15 benchmark data consisted of experimental data from Turkey Point Unit 3 and H.B. Robinson Unit 2. Samples from Turkey Point were collected from near the center of the fuel rod. Four samples from H.B. Robinson were obtained from various positions of a single rod while the other two were measured from a second pin.

The results from the Turkey Point benchmark averaged an error of 2.03% over all plutonium isotopes for all runs. However, ^{238}Pu was over-predicted by as much as 16%. ^{148}Nd was also benchmarked and had an error $\leq$5%, indicating that the assembly-averaged power history reasonably approximates the burnup of the assayed pin. ^{235}U was found on average to agree with experimental results within 3%. The experimental uncertainty was not recorded in the primary report.

The results for the H.B. Robinson benchmark were less accurate than Turkey Point. This is likely a result the specific assembly history; the H.B. Robinson assembly was irradiated for two cycles in two different locations in the core. During the first cycle only, the fuel pin was

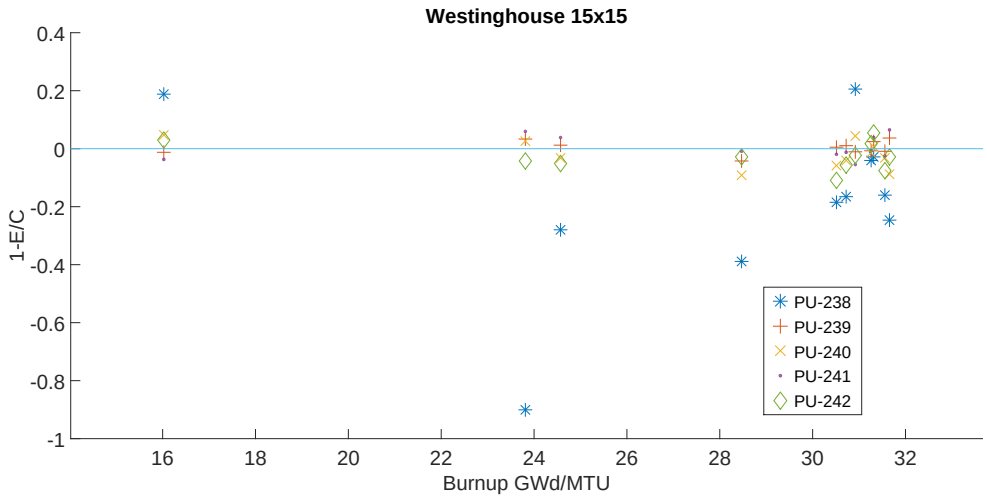

Figure 20: Westinghouse 15x15 plutonium isotopic benchmarks

adjacent to a burnable poison rod, which will significantly impact the shape of the local neutron spectrum; this burnable poison rod was not modeled (the rod was removed following the first cycle). Nonetheless, ^{235}U was typically within 4-5% of the measured value. Many of the plutonium isotopes resided within 10% of the experimental value. ^{238}Pu values were particularly inaccurate seeing error as high as 90%.

The experimental benchmark data for the Westinghouse 17x17 came from Takahama Unit 3. The assay collected 16 different samples, however, 5 of these are UO_2-Gd_2O_3 which were not considered. The eleven samples used were both on the edge of the assembly. There was an extended isotopic inventory conducted on the samples. Most of the calculated plutonium inventories were within 10% of the measured value, with many residing inside 5%. One sample, SF97-1, had relatively high error, around 20%. However, this is consistent with the previous validation study which produced plutonium inventories which were had 15-20% error [18].

Several different neodymium isotopes were benchmarked. Most of the isotopes showed good agreement and were within 5% of the experimental value. ^{142}Nd and ^{144}Nd had higher errors than the other isotopes, although ^{144}Nd was within 10%. ^{142}Nd data was not available for all samples. Cesium isotopes were also benchmarked and saw good agreement within 3-4%, indicating that that the assembly-averaged power history provides a reasonable approximation of the pin-specific burnup.

The Combustion Engineering benchmark benchmark was derived from data from Calvert Cliffs Unit 1. There were three samples from two different assemblies for a total of six samples. The concentration of soluble boron was known, but was not modeled. ^{148}Nd content and linear heat generation rates were available for each sample. At each axial location the linear burnup of time intervals was calculated as the product of the interval size and linear heat generation rate were summed for each cycle. The linear burnups were then normalized to the total burnups which

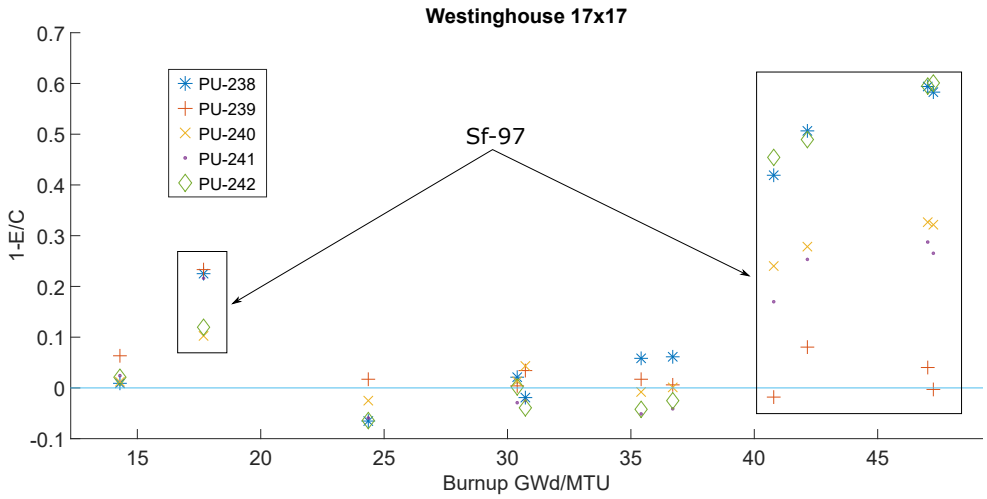

Figure 21: Westinghouse 17x17 plutonium isotopic benchmarks

were used in the simulation.

Major actinides for assembly D101 saw reasonable agreement, however, ^{238}Pu and ^{241}Pu were overpredicted with respect to the experimental value. This is likely due to the assayed pin which resided at the edge of the assembly. The flux shape of a pin at the edge of the assembly is different than an interior pin, which is not accounted for in this simplistic model.

The major actinide values for assembly D047 had good correspondence with measured values except for ^{238}Pu and ^{235}U, both of which were overpredicted. Additionally, all Nd isotopes for the three samples were within 5% of recorded values. The previous benchmark study indicated that the irradiation history was adjusted to achieve good results [18].

Eleven samples from Three Mile Island Unit 1 (TMI-1) were used to benchmark the unmodified performance of the Babcock & Wilcox 15x15 lattice. All of the samples originated from different axial positions of the same fuel rod. Uranium isotopic predictions were generally within 5-10% experimental values and similar to prior validation studies [18]. Plutonium isotopics were similar to previous studies, however, were quite inaccurate in some cases. Burnable poison rods were present for the first irradiation cycle, but were removed for the second cycle which were not modeled. In order to achieve good results and an accurate local environment, the previous benchmark study depleted nearest neighbor pins individually which was not performed for this study. The previous study achieved accuracy around 10-20% error for the plutonium isotopics. Neodymium saw excellent correspondence with experimental values typically having an error of only a few percent, indicating good agreement between the modeled and actual fuel burnup. The TMI-1 assay provided an extended isotopic comparison. Minor fission products such as Sm saw reasonable agreement within 10-12% of the experimental values. However, other fission products such as ^{155}Eu saw poorer correspondence with isotopic inventories 200% higher than experimental values.

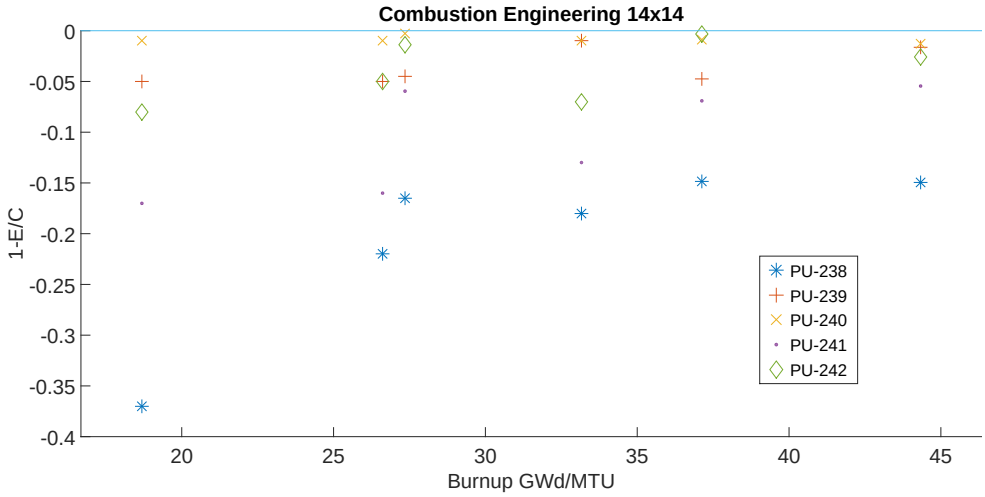

Figure 22: Combustion Engineering 14x14 plutonium isotopic benchmarks

Another five samples from TMI-1 were recently analyzed by ORNL [8]. Two rods in close proximity to a guide tube were assayed. The rods were present for two cycles, the first of which contained boron carbide rods which were not modeled. This resulted in uranium isotopics that ranged from a 14% overprediction to being as close as 5% depending on axial location. Plutonium isotopes generally reside within 10% of experimental values. This is likely due to a the absence of precise decay modeling. Additionally, the ORNL report provided results from a high-fidelity lattice transport calculation. The plutonium isotopics, when calculated with the burnable rods, were typically within 4-6% of experimental measurements. In this instance there is an increase in accuracy of about 5-7% when using the high-fidelity model. Uranium isotopics were overpredicted by 10-12%.

2.6.2 Multivariate analysis

This study also considers the use of PCA to analyze trends in large fuel assay sets. Previous work has been conducted that indicated that similar techniques can be used to determine reactor origin, either pressurized or boiling water reactor, and burnup of the fuel using nuclide concentrations as input data. Initial work has been generating a PCA model of the spent fuel assay as seen in Figure 24. Plutonium and uranium inventories were selected as the input data for the model due to their commonality across all experimental assays. The entire experimental data set of inventories across all assemblies was used to calibrate a PCA model. The calculated data resulting from the lattice physics simulations were used as validation data. This technique used as a tool to examine how the isotopics cluster in a reduced space. It is difficult to compare the difference between experimental and calculated values across several assemblies and many samples. This model enables a comparison based on cluster analysis. That is, for each isotope presented in the

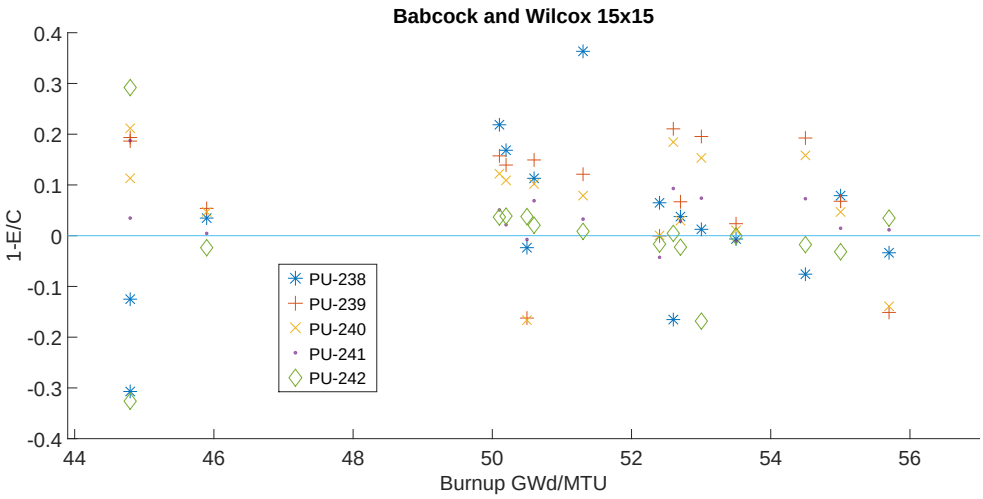

Figure 23: Babcock & Wilcox 15x15 plutonium isotopic benchmarks

plot, there was originally 39 features representing a measurement for each sample considered. It would be quite difficult to compare 39 calculated ^{235}U measurements against the corresponding experimental measurement. However, by using a dimensionality reduction technique such as PCA it is possible to compare the experimental and calculated values in a simple two-dimensional space.

The calculated major actinides fit within the uncertainty for the generated model. Many of the calculated major actinides lie close to their experimental counterpart in the principal component space. This would indicate that the inventories are similar and close together. However, other isotopes such as ^{234}U are not as close together. This would indicate that the calculated and experimental values are not, on average when considering all 39 samples, very close together. This is an expected behavior as it is quite difficult to accurately predict ^{234}U. It is currently unknown why ^{235}U loads differently on the first principal component. Since the first principal component captures 97% of the variance it is expected for most of the nuclides to have similar values for PC1 indicating they have similar linear variance. PC1 captures most of the variance which indicates that the linear variation of the major actinides is very similar, except for ^{235}U whose linear variation is quite different. It is likely that the reason ^{235}U loads differently in the reduced space is due to how the final inventory is calculated. While most actinide species slowly build in with burnup, ^{235}U is unique in that it depletes out over the course of the cycle.

A PLS (Partial Least Squares) study was generated using all of the calculated uranium and plutonium isotopics as the X block data. The burnup for each sample that was assayed was loaded as the Y block data set such that every observation in X had a corresponding burnup measurement in Y. The model was calibrated to find the maximum variation in the isotopics (X) that could be explained by the burnup (Y). Initial results show that 85% of the linear variation in the uranium and plutonium isotopics can be explained by the variation in burnup. This is

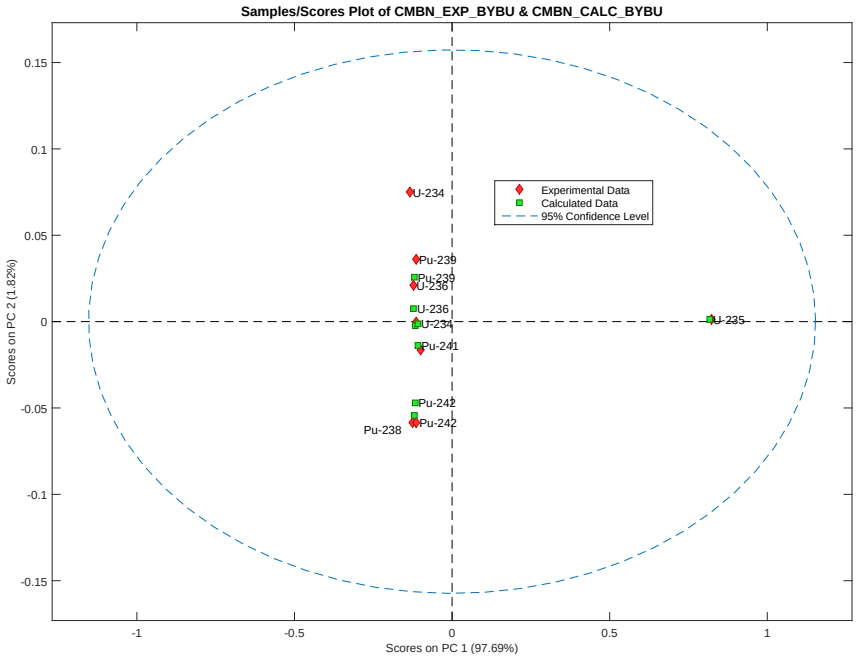

Figure 24: PCA model of experimental and calculated major actinide inventories

consistent with the observations made in the benchmark analyses. In cases where more advanced parameters, such as burnable poisons or the boron letdown curve, were not modeled, the accuracy of major actinides decreased by 5-15%.

2.6.3 Conclusions

Through the process of evaluating unmodified PWR templates used for ORIGEN reactor data library generation (matching only gross-level parameters typically used for reactor data library interpolation, such as initial enrichment and total assembly burnup), we have found that for many samples, reasonably accurate values for major plutonium species of interest (especially ^{239}Pu and ^{240}Pu) are obtained, generally within 5–10% of benchmark values on the basis of these factors alone, omitting detailed characteristics such as soluble boron letdown curves and burnable absorbers. In particular, we observed that predictions of plutonium isotopic species fared better for samples where the flux characteristics were closer to "assembly-average" conditions, such as being located far away from local features such as burnable absorber rods or water holes, both of which would adversely impact the local flux profile. These findings were confirmed by multivariate analysis techniques, which found that approximately 85% of the linear variation in uranium and plutonium isotopes could be explained by variations in burnup. Such a finding therefore places a rough upper bound to uncertainty introduced in using generic lattice templates to represent assembly-averaged isotopic inventories without consideration of cycle-specific features (such as

burnable poisons, adjacent assemblies, etc.)

2.7 Development of an ORIGEN-based reactor module for Cyclus

- **Targeted completion date:** July 2016
- **Task completion status:** 100%

The overall goal of this project component is the core deliverable of the overall project. The goal of this work is to deliver a physics-based reactor analysis capability for Cyclus capable of accurately evaluating a broad space of possible incoming fuel parameters. Particularly valuable envisioned use cases of this include assessments of reactor-based reuse of recovered actinide materials, including scenarios such as EG29 (wherein plutonium from fast reactors is fed back into thermal-spectrum critical reactors, such as the current light-water reactor fleet), as well as in the ability to assess characteristics such as the sensitivity of transition analysis scenarios (such as the transition from the current once-through cycle to more sustainable options relying on closing the fuel cycle).

Minimum necessary features for this archetype include the ability to access the full suite of Origen API layers to perform depletion and decay calculations with material streams. This in turn requires the ability to locate, process, and interpolate Origen reactor data libraries to perform the depletion calculation, while preferably also allowing the user the freedom to readily supply new reactor data libraries as needs arise to perform calculations for novel reactor types (e.g., fast-spectrum reactors, etc.)

Several of the Origen-related development tasks outlined previously in this report (e.g., generalized interpolation) are designed to support this overall effort. As of the last project performance period, the necessary infrastructure is sufficiently mature as to warrant beginning development on the reactor module itself. This has consisted of a multi-part effort designed both to develop the team's level of experience working with the Cyclus ecosystem as well as to begin developing the necessary infrastructure required to rapidly develop a working prototype. These efforts intended to support the main Cyborg development effort are detailed in the follow subsections.

2.7.1 Development of a storage facility archetype for Cyclus

In order to gain experience with Cyclus development (in preparation to develop the Cyborg reactor module for Cyclus), our group took on the development of a material storage facility archetype for Cyclus, to be included in the v1.3 release. This archetype is responsible primarily for holding material for a fixed period of time (specified by the archetype configuration) while allowing for capacity-based constraints (representing both annual material handling capacity as well total facility storage capacity). This archetype was likewise designed to employ the latest enhancements to the Cyclus Dynamic Resource Exchange (DRE), thus conveying valuable

practical experience in interfacing with the Cyclus kernel which was then parlayed directly into Cyborg development.

During this time period, the storage facility archetype was completed and approved by the Cyclus core development team for inclusion into the Cycamore module repository. As part of this process, a series of unit tests were created for the storage facility module in order to verify its correct functionality; these are described in Table 6.

Table 6: Unit tests developed for the `Storage` facility archetype to verify correct functionality

Test name	Purpose
`NoProcessTime`	Ensure the material is passed through in a single time step when the `residence_time` of the facility is set to 0 time steps.
`NoConvert`	Verify that the output material recipe is the same as the input material recipe when no radioactive decay is included.
`MultipleSmallBatches`	Test the facilitys ability to handle processing numerous material objects coming in at different times.
`ChangeCapacity`	Verify that changes to the throughput of the facility are reflected in its operation.
`TwoBatchSameTime`	Show that facility can handle multiple batches of material entering at the same time.
`ChangeProcessTime`	Verify that changes to the `residence_time` are reflected in the facility's operation.
`DifferentRecipe`	Ensure that the facility will accept any commodity recipe that is offered to it and not change its composition.

2.7.2 Development of Origen API bindings for Origen-based reactor module for Cyclus

A key component of the implementation of the Cyborg reactor module for Cyclus is in the development of an approrpriate binding layer between the Cyclus-facing archetype module code (responsible for handling the gross reactor archetype behavior, such as overall configuration, resource exchange within Cyclys, etc.) and the Origen API layer (which combines fuel cycle information such as cycle power, initial compositions, and reactor data library information to produce depleted concentrations). In order to keep the development process tractable, we have made the decision to employ a "binding layer" between Cyclus and Origen, with the intent of segregating Origen and SCALE-specific datatypes from those specific to Cyclus. This likewise enables our development effort to focus on testing reactor logic behaviors (i.e., the high-level behaviors of a reactor system expected of a reactor archetype) within the archetype while meanwhile minimizing departures from Cyclus conventions within the archetype itself. Meanwhile, the interface layer insulates Origen API calls from the need to understand Cyclus

data conventions; instead, data is passed to and from Cyclus and Origen using C++ primitive types and datastructures found in the standard library (e.g., `std::vector`, `std::map`, etc.). The binding layer provides all necessary translation of data to native types required by Cyclus and Origen, respectively.

This operation likewise folds in testing of the necessary Origen "builder's API," namely by developing a procedure for linking to the required Origen shared object library files from an out-of-source build configuraiton. At present, this work has been demonstrated through targeting the required Origen shared object libraries present on a shared system (i.e., based on a pre-release version of SCALE 6.2). At present, a prototype build system using CMake to locate required dependencies in a platform-independent fashion is presently functional on Linux and OSX-based systems (the same operating systems presently supported by Cyclus. In as much, we anticipate even with a delayed release of a separate "builder's API" package of Origen shared object library files, the current build configuration will be readily usable by external developers and users who at a minimum have access to the SCALE 6.2 binaries upon release; i.e., the current build system allows users to link against pre-compiled Origen library from outside the SCALE build system. To aid in this process, the automatically-generated Origen API documentation has been cleared for export control purposes and made publicly available online[1].

Fundamental to the design strategy of the CyBORG module is a modular separation of Cyclus-facing components (controlling the interactions with the material flows within the fuel cycle simulator environment) and the ORIGEN-facing components (governing the physics of material transformations within the reactor). This separation is achieved through the implementation of a Cyclus-ORIGEN interface layer, wherein material compositions and fuel cycle parameters (e.g., reactor power, cycle length, and fuel type) are passed in as C++ Standard Library container types (e.g., `std::vector`, `std::map`) and primitives like `int`, `float`, etc.

This calculation process is illustrated as Figure 25. Reactor parameters and materials are obtained from the Cyclus simulation as Cyclus-specific types (e.g., `Cyclus::Material`) and are passed to the Cyclus-ORIGEN interface as Standard Library types. The Cyclus-ORIGEN interface then produces an interpolated, problem-specific library from on-disk ORIGEN reactor data libraries and translates problem parameters into ORIGEN data containers for problem execution. Depleted compositions are then translated back to Standard Library types and returned to Cyclus to update the discharge material compositions.

By maintaining a strict separation between data types intrinsic to Cyclus and ORIGEN, this modularity allows for the incorporation of ORIGEN-based reactor analysis capabilities with minimal required knowledge of ORIGEN data types or conventions, decoupling implementation-specific details of ORIGEN-based depletion from the top-level fuel cycle parameters. In as much, the implementation of the CyBORG archetype itself is able to conform as much as possible to Cyclus conventions with minimal required deviations, thereby simplifying maintainability and lowering burdens to future developers. In similar fashion, the Cyclus-ORIGEN interface layer

[1] See `https://wawiesel.github.io/OrigenAPI-Demo/`

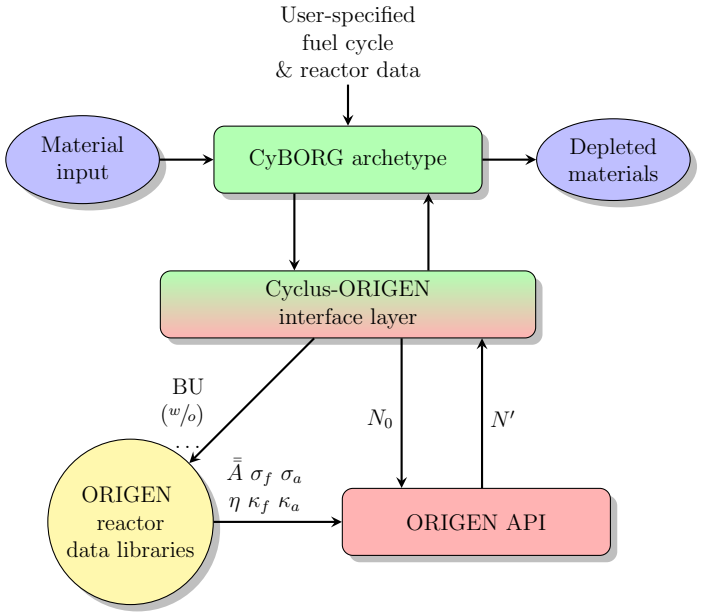

Figure 25: CyBORG design and execution flow. Reactor and fuel cycle data is passed through the Cyclus-ORIGEN interface to generate problem-specific reactor data used by ORIGEN, which returns depleted material information back to Cyclus.

affords developers the ability to easily develop new ORIGEN-based analysis capabilities within Cyclus as needs arise, such as modeling reactors with continuous feed/removal of fuel materials, flux-based irradiation of transmutation targets, and other physics-based applications.

Development work began in earnest on the API bindings near the end of the 2014-2015 performance period, with an initial release version now ready for public consumption. The binding layer code, as well as the CYBORG source code under development, is currently available at the CYBORG GitHub repository [22].

2.7.3 CyBORG features and capabilities

As presently implemented, the CYBORG reactor archetype for CYCLUS is capable of dynamically calculating fuel discharge recipes from all current ORIGEN reactor types included with the SCALE 6.2 release, comprised of 194 fuel and reactor types. CYBORG automatically interpolates burnup and initial composition information from the fuel recipe provided by CYCLUS; additional user inputs include optional interpolation "tags" that allow for the specification of specific features affecting the spectrum such as moderator density (for BWR fuel types), etc. CYBORG employs the generalized interpolation framework developed for ORIGEN in order to allow for future scalability of different reactor types and interpolation dimensions; for example, future libraries may include the actinide fraction as a reactor data library interpolation parameter for fast reactor

library variants.

With respect to the treatment of mass flows, CyBORG strives for physical realism as much as possible. Ergo, CyBORG depletes assemblies as discrete quanta via "batches" processed through the reactors, in which assemblies with a defined mass are transmuted per Origen calculations. For a given set of assemblies composed of the same initial composition, the depletion calculation need only be performed once across the entire simulation. This is accomplished by using Cyclus' simulation context to store ("cache") discharge fuel recipes "tagged" to a specific set of irradiation and initial composition conditions (i.e., a "hash"). Owing to this "hash-and-cache" strategy, the expense of calculating new discharge recipes is only incurred when a new set of irradiation or initial composition conditions are encountered (for example, the enrichment of fuel assemblies to the reactor changes, the reactor power changes, etc.) Meanwhile, because depletion calculations are performed on a batch / sub-batch basis, CyBORG can handle even such cases as heterogeneous fuel inputs (i.e., wherein more than one fuel composition is accepted by the reactor) as well as correctly adjust recipes for partial-length cycles (i.e., the final core within a reactor's life). In addition, CyBORG automatically calculates multi-cycle depletion calculations by using the total number of assemblies in the core and the number of assemblies per batch to calculate the number of cycles; future iterations will likewise implement sub-batching (i.e., wherein to maintain an average discharge burnup limit, a fraction of the assemblies are burned for one fewer cycle). As much as possible, the design of CyBORG is to obviate the need for user inputs by automatically inferring information from the simulation context (such as the reactor specifications, input fuel recipe, etc.)

A summary of the available user inputs for CyBORG is provided as Table 7.

Table 7: CyBORG user input options

Input	Required?	Default	Description
fuel_incommods	Y	—	Name of the fuel commodity(ies) in Cyclus requested by the reactor
fuel_recipes	Y	—	Input composition(s) / recipe(s) of fuel accepted by the reactor; used for calculating depleted fuel composition
fuel_prefs	N	1.0	Preference for different fuel input commodity types
spent_fuel	N	"spent_fuel"	Name of the discharged fuel commodity
power_name	N	"power"	Name of the power commodity produced by the reactor

Continued on next page

Table 7: CyBORG user input options

Input	Required?	Default	Description
POWER_CAP	Y	—	Total thermal power of the reactor (in MW); used for calculating discharge burnup (and depleted composition)
ASSEM_SIZE	Y	—	Mass of an individual assembly accepted by the reactor (kg)
N_ASSEM_CORE	Y	—	Total number of assemblies present in the core
N_ASSEM_BATCH	N	N_ASSEM_CORE	Number of assemblies per batch; determines number of irradiation cycles to use for depletion. (Defaults to all assemblies in the core).
N_ASSEM_FRESH	N	0	Number of fresh assemblies to keep on-hand (if available)
ASSEMBLY_TYPE	N	W17X17	Fuel assembly type used for Origen depletion calculations
N_ASSEM_SPENT	N	1E9	Number of spent fuel assemblies that can be stored on-site before reactor operations stalls (i.e., cannot deplete more assemblies)
CYCLUS_TIME	Y	–	Duration of a full irradiation cycle (excluding refueling time); number of simulation timesteps
REFUEL_TIME	Y	–	Refueling outage time between cycles (in number of simulation timesteps)
FUEL_TYPE	N	"UOX"	Used to determine which interpolation parameters will be used for depletion; i.e., "UOX" depletes on ^{235}U content, whereas "MOX" depletes based on initial ^{239}Pu fraction within the Pu vector and fractional Pu content. Options are: UOX, MOX, and "Other" (which does not calculate interpolation parameters based on initial composition, such as for CANDU assemblies).

Continued on next page

Table 7: CyBORG user input options

Input	Required?	Default	Description
lib_path	N	—	Path to Origen reactor data libraries.
assem_type	N	w17x17	Origen reactor data library to use for depletion calculations
core_power_frac	N	1.0	Fraction of the **total** core power provided by each fuel batch. (i.e., a fuel batch may be responsible for 50% of the core thermal power in cycle 1, 30% in cycle 2, and 20% in cycle 3); values are automatically normalized to 1.0. Used to calculate non-homogeneous cycle powers for depletion.

2.7.4 Validation testing of the CyBORG reactor module for Cyclus

In order to deploy the CyBORG module with confidence, we have developed an expansive set of unit tests and acceptance tests that verify the correct operation of the CyBORG module. The unit tests developed for CyBORG are detailed as Table 8.

In addition, a number of acceptance tests have been performed to verify that the CyBORG module performs depletion calculations in a manner substantially similar to those from standalone Origen calculations. Note that certain small differences should be expected due to the differences in the interpolation algorithms between ARP and Obiwan, however these differences should overall be nominal. A comparison of the calculated results for a representative PWR calculation are provided as Table 9.

As one observes from Table 9, CyBORG appears to correctly process interpolation and depletion calculations for a typical PWR depletion case; nominal differences are observed for certain nuclides with larger production chains, such as ^{241}Am and ^{243}Am, likely attributable to differences in the interpolation methods used in ARP and Obiwan. Further tests are being developed to verify the correct interpolation and depletion performance for representative BWR and MOX fuel calculations.

Table 8: Description of unit tests developed for the CyBORG module.

Test name	Functionality tested
libManipulation	Tests that Origen reactor data libraries can be correctly loaded
idTagManipulation	Tests for correct manipulation of tagged Origen reactor data libraries by the Cyclus / Origen interface layer.
parameterManpulation	Tests for correct manipulation of interpolable parameters for Origen reactor data libraries by the Cyclus / Origen interface layer.
interpolationTest	Tests that interpolation can be performed without errors / exceptions by CyBORG (does not test for correctness of the interpolated result)
materialTest	Tests that Cyclus / Origen interface layer correctly initializes an Origen material object for depletion
powerTest	Tests that powers can be correctly set and manipulated in CyBORG
solveTest	Tests that CyBORG can correctly perform a sample depletion calculation with interpolation of an Origen reactor data library
CorrectnessTest	Tests a sample depletion calculation against a known result (obtained from a standalone calculation)

Table 9: Validation test conducted for a Westinghouse 17x17 (PWR) assembly; 4.0% initial enrichment, 33,000 $\frac{\text{MWd}}{\text{MTU}}$ discharge burnup, comparing CyBORG to a standalone calculation using Origen (with ARP for reactor data library interpolation).

Nuclide	Origen mass %	CyBORG mass %	C/E (%)
^{238}U	93.47	93.47	0.01
^{235}U	1.155	1.155	0.07
^{239}Pu	0.590	0.590	0.01
^{236}U	0.488	0.488	-0.01
^{240}Pu	0.226	0.226	-0.05
^{241}Pu	0.143	0.143	-0.01
^{242}Pu	0.0484	0.0484	-0.03
^{237}Np	0.0465	0.0464	-0.12
^{238}Pu	0.0168	0.0168	0.11
^{243}Am	0.0089	0.0088	-0.63
^{239}Np	0.0080	0.0080	-0.03
^{241}Am	0.0042	0.0044	0.75

2.8 Development of a generalized method for compressed Origen reactor data libraries

- **Targeted completion date:** December 2017
- **Task completion status:** 70%

In addition to providing enhancements to post-processing and tracking capabilities, one particular need for using ORIGEN in embedded contexts such as the CYCLUS nuclear fuel cycle simulator is the ability to use a reduced nuclide set for specific application contexts. This need arises both in terms of optimizing for the performance of the ORIGEN depletion sequence (i.e., the inclusion of over 2,200 tracked nuclides entails over 54,000 nuclide transitions in the transition matrix) but also reducing the nuclide set to a more appropriate, tractable set such to not compromise the performance of the nuclear fuel cycle simulator.

The goal of this order reduction process is to preserve the accuracy of responses of interest (e.g., decay heat, activity, specific isotopic chains of interest, etc.) while eliminating transitions that otherwise minimally contribute to the problem dimension of interest. This order reduction process can be thought of in two complementary ways: first, in eliminating nuclide transitions that are otherwise insignificant to the timescale of interest (e.g., nuclides with half-lives on the order of nanoseconds when evaluating responses on the order of decades), and second in eliminating nuclides that themselves do not significantly contribute to the problem response of interest.

2.8.1 Theory of the order reduction approach

The general theory of this approach can be thought of as defining a response q_i, where . Here, N_i is the number density of isotopic species i, and w_i is a "weight" factor for this species corresponding to the response. For example, if the metric of interest is decay heat, the weight w_i can be thought of as the decay heat emitted (in watts) per decay. The system response would thus simply be the sum of the responses for each isotope, i.e.:

$$q = \sum_{i=1}^{\approx 2{,}200} w_i N_i \tag{5}$$

Thus, an acceptable order reduction (removal of nuclide transitions from the transition matrix) would be one in which the following condition is satisfied:

$$|q' - q| < \varepsilon \tag{6}$$

where ε is some very small tolerance factor. This relationship can likewise be extended over a particular time interval of interest, i.e.:

$$q = \int_{t_1}^{t_2} dt \sum_{i=1}^{\approx 2{,}200} w_i N_i(t) \tag{7}$$

Thus, in approaching the library order reduction, the goal is to preserve the system response of interest q while eliminating as many transitions as possible. For example, consider the following system (Table 10):

Table 10: A sample nuclear transition system to demonstrate transition compression techniques

Nuclide	w_i	Fission yield (Y_i)	N_i ($t = t_0$)
A	1.0E-4	2.5E-3	100
B	1.0E-4	1.0E-5	1
C	10	1.0E-3	1000

Here likewise, assume that nuclides A, B, and C are all produced both directly by fission, while "B" and "C" are also daughter products of "A,", i.e.

$$A \xrightarrow{\beta^-} B \xrightarrow{\beta^-} C \tag{8}$$

Here, is it clear that the response from nuclide "B" is small; therefore the response can simply be remapped as follows:

$$A \xrightarrow{\beta^-} C \tag{9}$$

Here, the fission yield of "C" would adjusted accordingly (i.e., the direct yield of nuclide "B" would be added to nuclide "C"), thus preserving the total mass balance and accumulated yield. Similarly, were nuclide "A" removed, the transition to "C" (via fission yield) would simply be adjusted to include the accumulation from A. For example, this might be appropriate for a very short-lived transition over a long time period (e.g., looking at the decay precursors to ^{131}Xe, such as ^{131}I, ^{131}Te, ^{131}Sb, ^{131}Sn, and ^{131}In. Given that most of the decay parents of ^{131}Xe are exceptionally short-lived, it would be appropriate under this scheme to eliminate these parents, consolidating the fission yields directly into a longer-lived parent like ^{131}I at minimal cost to problem accuracy.

Similarly, "stranded" nuclides (i.e., nuclides for which any transitions to nuclides significant to the problem have been eliminated) can thus be safely eliminated from the problem with minimal loss of fidelity.

Here, the intent is to develop an approach which is generalizable (i.e., based on a user-provided response) while also rigorous (in order to preserve the solution accuracy). Such an approach of moving from general to specific libraries allows for this general capability, affording users the ability to select different nuclide sets based on the problem response of interest. Meanwhile, this type of order reduction will allow ORIGEN to be executed faster within CYBORG while operating with a smaller memory footprint (both in terms of ORIGEN execution as well as the size of the nuclide set propagated throughout the fuel cycle calculation). Thus, this capability will serve as an essential prerequisite task to the final version of CYBORG.

2.8.2 Implementation strategy

Implementation of a rigorous transition system reduction relies first upon the ability to create a "round-trip" system to recreate the full system of nuclear transitions tracked by ORIGEN. This includes reaction-based transitions (e.g., (n,γ), (n,α), (n,p), etc.), fission-induced transitions (i.e., production of nuclides directly from fission reactions), and decay reactions (including alpha and beta decay reactions).

This system of recreating a fully-specified transition system relies first on populating a transition system object (of class `TransitionSystem`) based on available fundamental nuclear data from AMPX master library data (i.e., decay data, fission yields, and reaction cross-sections, which when combined with a scalar flux, are used to produce reaction rates). Here, `TransitionSystem` is a general container designed to represent the relationships of nuclides via different transition channels (reaction-based, decay-based, and yield-based). Presently, the `TransitionSystem` architecture is oriented primarily toward allowing users to update rigorously update reaction cross-sections on a library by reconstructing a subset of the transition system and propagating changes to reaction cross-sections appropriately to all reaction products. The challenge here is therefore in generalizing this approach to reconstruct the **entirety** of the system from an on-disk compressed transition matrix, combining this with nuclear data from AMPX to create a fully-expanded transition system from which the transition channels can be more rigorously selected and edited.

Here, a challenge is in the fact that information is lost during the current process of creating a collapsed, one-group transition system from multi-group transport calculations. (i.e., in the ordinary sequence of ORIGEN reactor data library creation, 2-D lattice physics calculations are used to calculate the shape of the neutron flux at each timestep. This flux is then used to weight all of the reaction cross-sections to produce one-group cross-sections and thus a transition matrix used by ORIGEN to calculate depletion inventories.) During the collapse, information is about reaction and decay types is discarded (specifically, ENDF MT numbers pertaining to individual decay types), requiring to be regenerated at this step in order to produce the full transition system. This process of reconstructing the transition system has proven unexpectedly challenging and thus has slowed down development on this objective.

Presently, we have demonstrated the reduction of a full transition system from an on-disk ORIGEN reactor data library given a user-specified problem metric (e.g., decay heat), succesfully employing the ORIGEN TRANSITIONSYSTEM methods to recreate a full representation of the transition matrix (i.e., production and removal pathways for each nuclide), systematically identifying and removing nuclides of negligible consequence. This work was presented at the recent M&C 2017 conference.

From here, the following reduction strategies have been identified to reduce the ORIGEN library size (and thus memory footprint for calculations):

1. **Consolidation of Origen sublibrary nuclides**: This consists of taking the union of nuclides found across multiple ORIGEN sublibraries (i.e., light elements, actinides, fission products) and consolidating them into one sub-library. Examples of this would include

light elements like Gd and Sm (found in light element and fission product sublibraries), He (found in all three sublibraries, due to alpha decay and tertiary fission), etc. This reduction is expected to produce no difference in the actual "responses" (e.g., decay heat, total inventory, etc.); it is simply a removal of redundancy intended to streamline the data library itself (however this alone would lead to substantial savings).

2. **Removal of trace nuclide concentrations**: This step would eliminate nuclides (and their transitions) with time-weighted atom fractions less than some tolerance ε. Because this is taken over the total time domain of the problem, it is not expected to introduce adverse effects on the problem solution (although this will be validated). However, this is expected to remove many short-lived activation products (present only at trace levels) and extreme neutron-rich fission products (produced only very rarely from fission).

3. **Response-based removal of nuclides and transitions:** This process would now employ the response-based removal outlined in Equations 6 and 7. i.e., nuclides can be evaluated by the fractional production of the response of interest:

$$R_p^i(t) = \frac{w_i n_p(t) \cdot a_p^i(t)}{\sum_p n_p(t) \cdot a_p^i(t)} \tag{10}$$

Here, p is the parent nuclide index, $n_p(t)$ is the concentration of the parent nuclide at time t, w_i is the daughter nuclide response factor (e.g., decay heat in watts per decay, gamma energy release per decay in MeV, etc.), and $a_p^i(t)$ is the transition coefficient for the production of nuclide i from p. It is in this step where many of the actual *transitions* within the system are expected to be removed.

4. **Redistribution of yields for short-lived fission products:** This process would involve setting a screening criteria (based on a minimum decay constant and fraction of production of fission; e.g., "nuclides with half-lives under 1 hour with production from fission accounting for $\geq$ 99% of the nuclide's production"). Yields for these nuclides would be directly redistributed to daughter species. As previously, this step would be carefully validated to ensure minimal loss of fidelity.

The process as currently implemented is most easily understood as the flow diagram conveyed in Figure 26. One will observe that the present process is an *iterative* process of removals, in which the contribution threshold applied for determining the nuclide removal cutoff is adjusted to meet the global error condition.

2.8.3 Example transition system reduction

An example of a transition system reduction is illustrated as Figure 27. Here, the original system of 2237 nuclides is reduced to a system of around 300-500 nuclides based upon the contribution

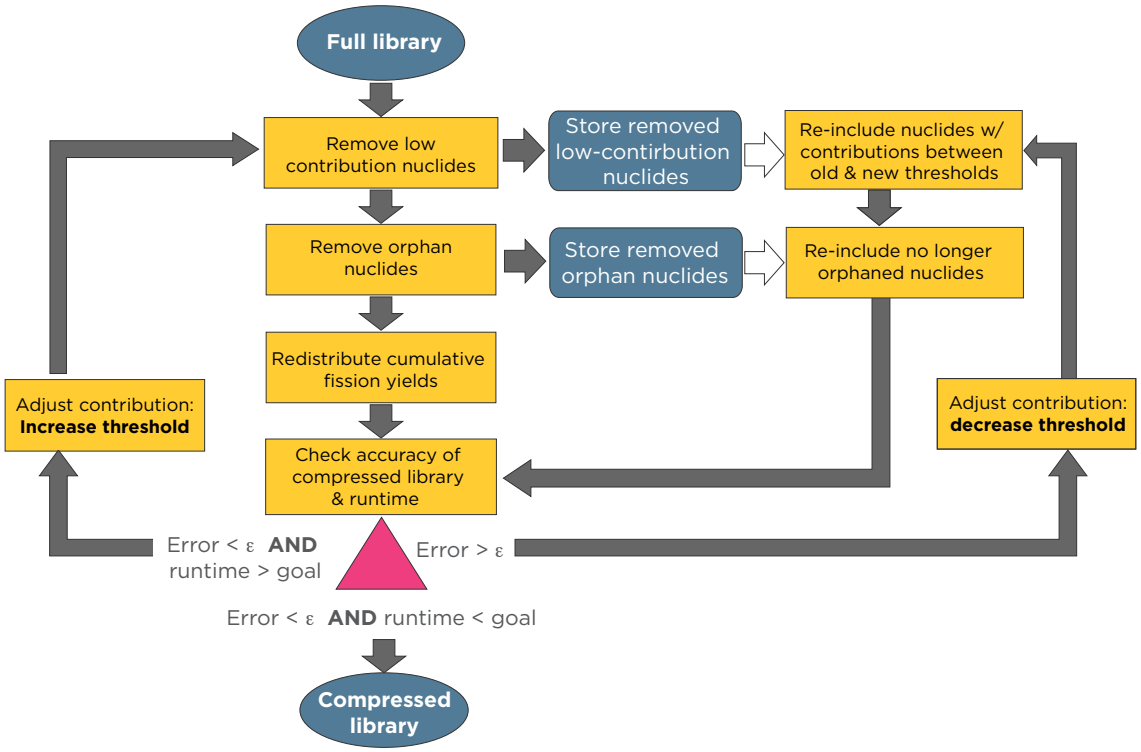

Figure 26: Flow diagram for the process of nuclide identification and removal for developing the reduced transition system for ORIGEN reactor data libraries.

to the final discharge mass. Of these reductions, over 60% of the total removals occurred in the fission product library, primarily arising from short-lived nuclides with low capture cross-sections and few connected transitions. As a result, their removal introduces very little error into the final result. In addition, large ranges of low-Z nuclides are eliminated corresponding to those nuclides which have overall low direct fission yields.

Based upon prior performance benchmarks of manually-reduced transition system matrices, a rough performance gain as indicated in Table 11 can be expected.

As is evident, higher removal thresholds (i.e., raising the threshold of the contribution under which a nuclide can be removed from the system) decreases the problem runtime. wherein the runtime appears to reduce roughly in proportion to the decrease in the number of transitions; however, above thresholds of around 1 ppm, the problem runtime does not substantially decrease while the error introduced precipitously increases. As such, a removal threshold of around 1 ppm for mass-based metrics appears to be an appropriate threshold, reducing the number of nuclides by about 50% and the transitions and problem runtime by just over 61%.

Table 11: Relative performance of ORIGEN depletion calculations based on transition matrix size.

Removal threshold	Nuclides remaining	Transitions remaining	Final error (% mass)	Problem runtime (ms)
10^{-4}	523	10,823	3.83	41
10^{-5}	1,083	18,785	0.336	80
10^{-6}	1,140	20,969	0.060	87
10^{-7}	1,193	23,051	0.057	94
0	2,237	54,331	0	223

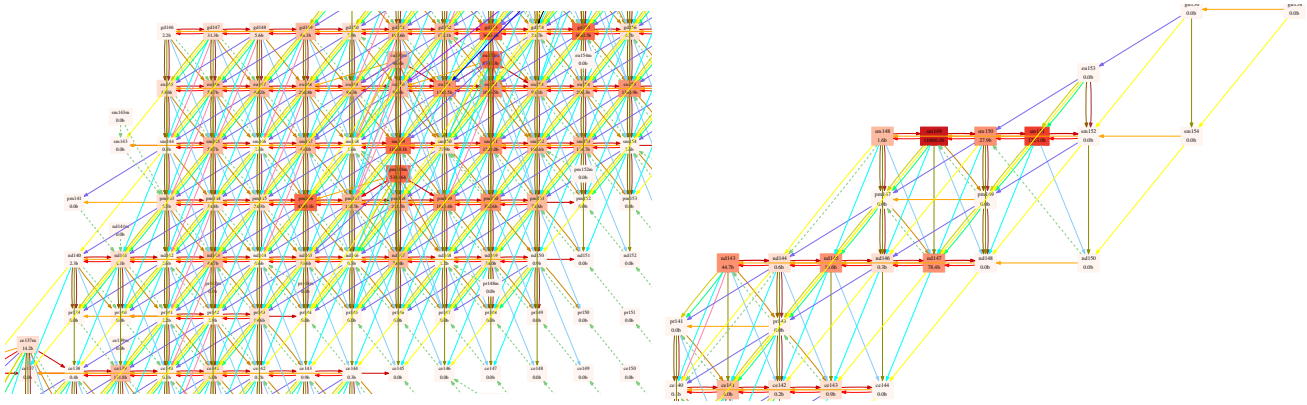

(a) Original transition system for Z = 58-64 & A = 137-156

(b) Reduced transition system for Z = 58-64 & A = 137-156

Figure 27: Subset of the full (left) and reduced (right) ORIGEN reactor data transition matrices.

2.8.4 Graph theory-informed approach

Current development efforts on a lossy compression algorithm for ORIGEN reactor data libraries is focused on implementing a graph theory-informed approach. In this formulation, the nuclide transition matrix is explicitly cast into a graph form, illustrated as Figure 28. Here, each nuclide represents a graph "node," wherein gains and removals from each nuclide (representing activation, decay, etc.) can be represented as pathways connecting each node. In as much, the treatment of the system reduction can be accomplished using well-established graph optimization algorithms.

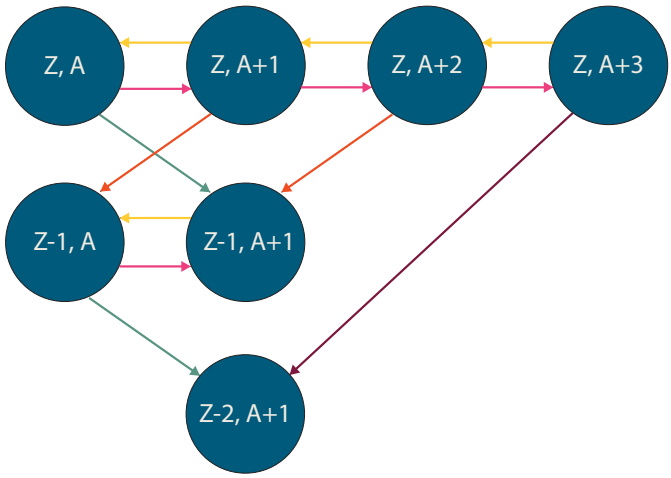

Figure 28: Representation of a transition system as a Graph Theory formulation

The advantage of a graph theory-based approach is thus twofold. In addition to leveraging well-established optimization techniques for reducing the number of nuclides and transitions in the system, a graph-based approach maximally preserves the physical representation of the system. While numerous approaches have been proposed to achieve reductions in the size of the nuclide transition matrix (e.g., through the introduction of basis functions, PCA, and other functionalization-based approaches), this approach differs in that what fundamentally results is a map of nuclide-to-nuclide transitions.

The scope of this work will continue beyond the funded period of this grant but it is planned that the resulting methods will be incorporated into future releases of the SCALE code system.

Taken together, the outlined plan has the potential to create application-specific streamlined libraries to enable much faster physics-based depletion calculations, thus minimizing the computational penalty for pursuing physics-based methods within fuel cycle simulations.

3 Overall project deliverables

3.1 Main project deliverables

3.1.1 Development and Validation of the Nuclear Fuel Inventory Module for Cyclus (Cyborg)

During the previous reporting period, progress on the CYBORG reactor module has focused chiefly upon developing the in-house experience in developing archetypes for use with CYCLUS. This includes development of a fully-compliant storage facility archetype designed to simulate time-limited storage of commodities (such as spent fuel, separated actinides), etc. In the implementation of this archetype, where possible we have pursued as rigorous as possible of a treatment of materials, including the option for discrete material handling, i.e. wherein received materials are treated as discrete unit quanta, such a fuel assembly, spent fuel cannister, etc. This treatment strategy allows for future use of CYCLUS in a variety of agent-bases scenarios, including movement of batched materials (e.g., movement of spent fuel contained in storage and transportation casks, wherein it is assumed these are indivisible mass units). The alternative to this, also supported by the storage facility archetype, is in continuous treatment of material flows - i.e., wherein the archetype will receive and send out material in arbitrarily-divided mass flows (this could be best envisioned in the context of continuous processes, such as UF_6 from a conversion plant, enriched uranium from an enrichment plant, MOX powder from a reprocessing plant, etc.).

This experience has proven tremendously useful in beginning development of the CYBORG reactor module, which is as of the end of the previous reporting period in the early stages of development. At present, this development is currently in early prototyping and development stages, focusing on producing a working minimal viable demonstration version capable of taking material from the CYCLUS Dynamic Resource Exchange, converting this material into a form usable by ORIGEN, locating and correctly interpolating a user-specified reactor data library, performing material depletion and decay, and then returning the isotopic inventories to CYCLUS in a form usable by the simulation (i.e., conversion back to a CYCLUS `Material` type).

Upon development of a minimal feature set, we anticipate developing more sophisticated features, including the ability to handle more complex user-defined cycles (e.g., variable powers by cycle to simulate the movement of an assembly through the core throughout multiple batches), the ability to accept multiple input streams (including multiple enrichments of UO_2 fuel or even mixtures of UO_2 and MOX fuel) and handle multiple output streams, and finally the investigation of appropriate interpolation parameters for advanced reactor types (in order to support physics-based transition analyses).

3.1.2 Enhancements to Origen to support the Nuclear Fuel Inventory Module

At the time of this reporting period, all of the required infrastructure enhancements to ORIGEN to support the development of the Nuclear Fuel Inventory Module (CYBORG) have been completed

and are scheduled for inclusion in the upcoming SCALE 6.2 release. This means that upon the public release of SCALE 6.2, external users will be able to compile CYBORG against the ORIGEN shared object libraries distributed with SCALE (including binary-only distributions that do not include SCALE source code), thus allowing CYBORG to function as a quasi-export-controlled module, in that the actual implementation details of ORIGEN functions are not exposed to the user. (i.e., the ORIGEN interface layer accesses functions declared in the ORIGEN header files and libraries, but the actual source code need not be compiled by the user or exposed to them).

A subset of these enhancements to support CYBORG development include:

1. Self-describing ORIGEN reactor data libraries (to facilitate generalized interpolation) via on-library "tags"
2. Generalized N-dimensional interpolation through the OBIWAN command-line tool and API
3. Generalized nuclide unit conversions through the ORIGEN `ConcentrationConverter` class (allowing unit conversions to different response types, including mass, heat, activity, etc.)
4. The ability to locate, select, and interpolate ORIGEN on-disk reactor data libraries directly through ORIGEN API calls

Taken together, these capabilities represent a powerful toolkit for future developers beyond application to the CYBORG physics-based reactor module. These capabilities are believed to be sufficient to fully leverage ORIGEN-based depletion methods within the CYBORG archetype.

3.1.3 Modernized Origen reactor data libraries and interpolation capabilities

As part of this project (as well as work occurring in parallel to this project), a series of modernized ORIGEN reactor data libraries were developed, spanning 194 different fuel types. Contributions specific to this project include the development of modernzied CANDU PHWR reactor data libraries. In addition, ongoing work is focused on the development of a generalized set of libraries for LMFBR fast-spectrum assemblies, comprising driver and blanket fuel, including development of appropriate interpolation parameters.

In addition, a fully generalizable interpolation framework has been developed to afford the use of new interpolation dimensions for ORIGEN reactor data libraries. The intended use of this capability is to afford modelers the ability to evaluate new effects such as average soluble boron concentrations as well as being able to consider different interpolation dimensions which may be appropriate to advanced reactor fuel types, such as the average actinide fraction within the fuel, etc. The resulting generalized interpolation capability has likewise lead to the development of ORIGEN reactor data libraries that are "self-describing," enhancing future portability.

While not completed within this workscope, plans call for the development of a consolidated "ORIGEN binary archive" format which will allow for consolidated ORIGEN reactor data libraries by assembly / reactor type, reducing both the (considerable) on-disk footprint (by eliminating

redundant information between libraries) as well as substantially reducing file I/O burdens, thereby increasing the performance of the CyBORG module. Present plans call for targeting the SCALE 6.3 release for this feature.

3.1.4 Problem-dependent Origen reactor data library compression for improved depletion performance

A thrust of this project which will continue on beyond the project conclusion is the development of a problem-dependent lossy compression algorithm for Origen reactor data libraries. The objective of this algorithm is to identify the nuclides and transitions which are essential to calculating a user-specified problem metric of interest, such as final decay heat at a given time, radiotoxicity, activity, etc. By developing a generalized compression algorithm, it is therefore possible to substantially reduce the calculation time required for depletion calculations, minimizing the impact of including physics-based depletion within larger frameworks such as Cyclus. This feature is anticipated to yield further benefits to ongoing NEAMS projects as well by allowing for the efficient generation of reduced libraries for depletion calculations within fuel performance simulations such as the MOOSE toolkit.

At present, work is ongoing to develop a graph theory-informed library reduction approach. Upon completion, these methods will be included into a future SCALE code release.

3.2 Journal publications

1. N. T. Shoman and S. E. Skutnik, "Development of modern CANDU PHWR cross-section libraries for SCALE," *Nuclear Engineering and Design*, 302(A), pp. 56-67, June 2016 `http://dx.doi.org/10.1016/j.nucengdes.2016.04.007`

2. S. E. Skutnik, "Proposed re-evaluation of the ^{154}Eu thermal (n,γ) capture cross-section based on spent fuel benchmarking studies," *Annals of Nuclear Energy*, 99, pp. 80-107, Jan. 2017; `http://dx.doi.org/10.1016/j.anucene.2016.09.003`

3.3 Conference publications

1. S. M. Richards and S. E. Skutnik, "Problem-Dependent ORIGEN Library Compression to Increase Computational Efficiency," *M&C 2017 - International Conference on Mathematics and Computational Methods Applied to Nuclear Science & Engineering*, Jeju, Korea, April 2017

2. S. E. Skutnik "Re-evaluation of the ^{154}Eu thermal capture cross-section based on spent fuel benchmarking studies," *M&C 2017 - International Conference on Mathematics and Computational Methods Applied to Nuclear Science & Engineering*, Jeju, Korea, April 2017

3. S. E. Skutnik and N. T. Shoman, "Re-evaluation of the ^{154}Eu thermal capture cross-section based on spent fuel benchmarking studies," *PHYSOR 2016*, Sun Valley, ID, May 2016.

4. N. C. Sly, S. E. Skutnik, and W. A. Wieselquist, "Portable Reactor Data Library Interpolation via Self-Describing ORIGEN Libraries," *PHYSOR 2016*, Sun Valley, ID, May 2016.

5. N. T. Shoman and S. E. Skutnik, "Verification and Validation of New Unmodified SCALE PWR Lattice Templates," *PHYSOR 2016*, Sun Valley, ID, May 2016.

6. S. E. Skutnik, N. C. Sly, and J. L. Littell, "Development of an ORIGEN-based reactor analysis module for Cyclus," *Transactions of the American Nuclear Society*, 115(1), pp. 299–301, November 2016

7. N. T. Shoman and S. E. Skutnik, "Verification and Validation of New Unmodified SCALE PWR Lattice Templates," *Transactions of the American Nuclear Society*, 113(1), pp. 1306–1309, October 2015

8. N. T. Shoman and S. E. Skutnik, "Development of Modern CANDU PHWR Cross-Section Libraries for SCALE," *Transactions of the American Nuclear Society*, 113(1), pp. 178–181, October 2015

9. N. C. Sly, S. E. Skutnik, and W. A. Wieselquist, "Portable Reactor Data Library Interpolation via Self-Describing ORIGEN Libraries," *Transactions of the American Nuclear Society*, 113(1), pp. 368–371, October 2015

4 Participants & collaborating organizations

4.1 Graduate students supported

4.1.1 Nathan Shoman

- **Project role:** Graduate student (M.S.)
- **Nearest person-months worked:** 18
- **Contributions to project:** Mr. Shoman has performed work in developing and testing the CANDU PHWR fuel lattice templates along with performing validation studies on unmodified PWR fuel assembly lattice templates.

4.1.2 Jennifer Littell

- **Project role:** Graduate student (M.S.)
- **Nearest person-months worked:** 16
- **Contributions to project:** Ms. Littell developed the `Storage` facility archetype for Cyclus and has been responsible for leading the initial Cyclus-facing development for the Cyborg Origen-based reactor module for Cyclus.

4.1.3 Nicholas Sly

- **Project role:** Graduate student (Ph.D.)
- **Nearest person-months worked:** 36
- **Contributions to project:** Mr. Sly has been chiefly responsible for leading efforts to develop the generalized Origen reactor data N-dimensional interpolation framework, including development of the `TagManager` class as well as providing supporting development for the Obiwan command-line interpolation utility. He has also lead the development of the Cyclus-Origen API interface layer needed to access Origen depletion APIs through Cyclus.

4.1.4 Scott Richards

- **Project role:** Graduate student (Ph.D.)
- **Nearest person-months worked:** 24
- **Contributions to project:** Mr. Richards has been primarily responsible for the development of a generalized, rigorous method to compress Origen reactor data libraries (i.e., number of transitions within the transition matrix) to provide problem-specific runtime performance enhancements while sacrificing minimal fidelity.

4.2 Partner organizations

4.2.1 Oak Ridge National Laboratory

- **Location:** Oak Ridge, TN
- **Contributions to project:** ORNL is responsible for collaborative research on this project, including reviewing all modifications to the ORIGEN code. They have likewise contributed numerous enhancements to the ORIGEN code designed to support this project, including necessary changes to the ORIGEN API and the development of a new keyword-based input for ORIGEN standalone calculations. They have also been responsible for the development of the medium-fidelity "on-the-fly" cross-section calculation and depletion capability (via TDEPL-1D).

5 Project impacts

The implementation of this project carries with it a number of potential broader impacts beyond the immediate deliverable of the reactor module for Cyclus. In particular, improvements to Origen will be available to all users of the upcoming SCALE 6.2 release; of these, most prominent among them will be the new text-based Origen input format (dramatically simplifying the user experience). Additionally, while the migration to fully self-describing Origen reactor data libraries is not yet complete, it is anticipated that this development will greatly simplify the process of creating and managing new reactor data types for Origen depletion calculations.

In addition, preparation and execution of this project has lead to useful contributions back to Cyclus, including the storage facility archetype as well as build system improvements to the Cyclus code base (to facilitate better interoperability across operating systems).

Further, an unexpected impact of this project has been in the discovery of possible discrepancies in the nuclear data evaluations for ^{154}Eu and ^{154}Sm, the former of which is especially significant from a spent fuel storage and monitoring perspective (given that ^{154}Eu is a relatively prominent gamma-emitting nuclide, important to both shielding/dose calculations for spent fuel storage as well as being a burnup indicator for non-destructive analysis). Both nuclides are likewise significant from a burnup credit perspective (^{154}Sm from its indirect relationship to ^{155}Eu, a strong neutron absorber, which is produced from neutron capture by ^{154}Sm and subsequent β^- decay by short-lived ^{155}Sm). Our studies showed that changes to these evaluations show significant impacts on highly-thermalized systems (like CANDU reactors) and may manifest noticeable impacts on other light-water / thermal systems (such as a typical PWR).

This project has likewise supported the training of several students, including two masters students (both of whom graduated and left project in Spring 2016) and two Ph.D. students.

References

[1] V. A. Anufriev, S. I. Babich, A. G. Kolesov, V. N. Nefelov, V. A. Poruchikov, V. A. Safonov, A. P. Chetverikov, V. S. Artamonov, R. N. Ivanov, and S. M. Kalebin. Measurement of the total neutron cross sections of ^{153}Eu, ^{154}Eu, and ^{155}Eu. *Soviet Atomic Energy*, 46(3):182–185, 1979.

[2] M.S. Basunia, R.B. Firestone, Zs. Révay, H.D. Choi, T. Belgya, J.E. Escher, A.M. Hurt, M. Krtička, L. Szentmiklósi, B. Sleaford, and N.C. Summers. Determination of the ^{151}Eu(n,γ)^{152m1,g}Eu and ^{153}Eu(n,γ)^{154}Eu Reaction Cross Sections at Thermal Neutron Energy. *Nuclear Data Sheets*, 119:88–90, May 2014.

[3] M.B. Chadwick et al. ENDF/B-VII.0: Next Generation Evaluated Nuclear Data Library for Nuclear Science and Technology. *Nuclear Data Sheets*, 107(12):2931–3060, December 2006. Evaluated Nuclear Data File ENDF/B-VII.0.

[4] M.B. Chadwick et al. ENDF/B-VII.1 Nuclear Data for Science and Technology: Cross Sections, Covariances, Fission Product Yields and Decay Data. *Nuclear Data Sheets*, 112(12):2887–2996, 2011. Special Issue on ENDF/B-VII.1 Library.

[5] Cross-Section Evaluation Working Group. ENDF/B-VI Summary Documentation. Technical Report BNL-NCS-17541 (ENDF-201), 1998. Data Library ENDF/B-VI, update 1998, by the U.S. National Nuclear Data Center on behalf of the Cross-Section Evaluation Working Group.

[6] I. C. Gauld. Mox cross-section libraries for origen-arp. Technical Report ORNL/TM-2003/2, Oak Ridge National Laboratory, July 2003.

[7] I. C. Gauld, P.A. Carlson, and K.A. Litwin. Production and Validation of ORIGEN-S Cross-Section Libraries for CANDU Reactor Fuel Studies. Technical Report RC-1442; COG-I-95-200, Whiteshell Laboratories, October 1995.

[8] I. C. Gauld, J. M. Giaquinto, J. M. Delashmitt, J. Hu, G. Ilas, T. J. Haverlock, and C. Romano. Re-evaluation of spent nuclear fuel assay data for the three mile island unit 1 reactor and application to code validation. *Annals of Nuclear Energy*, 87(2):267–281, January 2016.

[9] I. C. Gauld, J. M. Giaquinto, J. S. Delashmitt, J. Hu, G. Ilas, T. J. Haverlock, and C. Romano. Re-evaluation of spent nuclear fuel assay data for the Three Mile Island unit 1 reactor and application to code validation. *Annals of Nuclear Energy*, 87, Part 2:267 – 281, 2016.

[10] I. C. Gauld and K. A. Litwin. Verification and Validation of the ORIGEN-S Code and Nuclear Data Libraries. Technical Report RC-1429 / COG-I-95-150, Atomic Energy of Canada Limited (AECL), August 1995.

[11] I. C. Gauld, G. Radulescu, G. Ilas, B. D. Murphy, M. L. Williams, and D. Wiarda. Isotopic Depletion and Decay Methods and Analysis Capabilities in SCALE. *Nuclear Technology*, 174(2):169–195, May 2011.

[12] Richard J. Hayden, John H. Reynolds, and Mark G. Inghram. Reactions induced by slow neutron irradiation of europium. *Phys. Rev.*, 75:1500–1507, May 1949.

[13] G. Ilas and I. C. Gauld. Analysis of Experimental Data for High-Burnup PWR Spent Fuel Isotopic Validation–Vandellós II Reactor. Technical Report NUREG/CR-7013 / ORNL/TM-2009/321, U.S. Nuclear Regulatory Commission (NRC), January 2011.

[14] G. Ilas, I. C. Gauld, F. C. Difilippo, and M.B. Emmett. Analysis of Experimental Data for High Burnup PWR Spent Fuel Isotopic Validation–Calvert Cliffs, Takahama, and Three Mile Island Reactors. Technical Report NUREG/CR-6968 / ORNL/TM-2008/071, U.S. Nuclear Regulatory Commission (NRC), February 2010.

[15] G. Ilas, I. C. Gauld, and B. D. Murphy. Analysis of Experimental Data for High Burnup PWR Spent Fuel Isotopic Validation–ARIANE and REBUS Programs (UO_2 Fuel). Technical Report NUREG/CR-6969 / ORNL/TM-2008/072, U.S. Nuclear Regulatory Commission (NRC), February 2010.

[16] L. C. Leal, O. W. Hermann, S. M. Bowman, and C. V. Parks. Arp: Automatic rapid process for the generation of problem-dependent sas2h/origen-s cross-section libraries. Technical Report ORNL/TM-13584, Oak Ridge National Laboratory, April 1998.

[17] Said F. Mughabghab. *Atlas of Neutron Resonances, Fifth Edition: Resonance Parameters and Thermal Cross Sections. Z=1-100*. April 2006.

[18] G. Radulescu, I. C. Gauld, and G. Ilas. SCALE 5.1 predictions of PWR spent nuclear fuel isotopic compositions. Technical Report ORNL/TM-2010/44, Oak Ridge National Laboratory, 2010.

[19] Toshiaki Sekine, Shin-Ichi Ichikawa, and Sumiko Baba. Triple Neutron Capture of ^{153}Eu in a Reactor: The Cross Sections of ^{154}Eu and ^{155}Eu. *International Journal of Radiation Applications and Instrumentation. Part A. Applied Radiation and Isotopes*, 38(7):513–516, 1987.

[20] N. T. Shoman and S. E. Skutnik. Development of modern CANDU PHWR cross-section libraries for SCALE. In *Transactions of the American Nuclear Society*, volume 113, pages 178–181, October 2015.

[21] Nathan T. Shoman and Steven E. Skutnik. Development of modern CANDU PHWR cross-section libraries for SCALE. *Nuclear Engineering and Design*, 302, Part A:56 – 67, 2016.

[22] S. E. Skutnik, N. C. Sly, and J. L. Littell. CyBORG: Cyclus-Based ORIGEN code repository. `https://github.com/sskutnik/cyborg/`.

[23] Steven E. Skutnik. Proposed re-evaluation of the ^{154}eu thermal (n, γ) capture cross-section based on spent fuel benchmarking studies. *Annals of Nuclear Energy*, 99:80 – 107, 2017.

[24] V .P. Vertebnyj, P. N Vorona, A. I. Kal'chenko, V. G. Krivenko, and V. A. Pshenichnyj. Neutron resonances of the radioactive nuclides eu-154 and eu-155. *Vop. At.Nauki i Tekhn., Ser. Yadernye Konstanty*, 5(49):16, 1982.